ELSEVIER

Marine Geology 237 (2007) 71 – 96

MARINE GEOLOGY
INTERNATIONAL JOURNAL OF MARINE GEOLOGY, GEOCHEMISTRY AND GEOPHYSICS

www.elsevier.com/locate/margeo

Marine geology of the Quaternary Bass Canyon system, southeast Australia: A cool-water carbonate system

J.K. Mitchell *, G.R. Holdgate, M.W. Wallace, S.J. Gallagher

School of Earth Sciences, The University of Melbourne, VIC, 3010, Australia

Received 16 November 2005; received in revised form 16 October 2006; accepted 23 October 2006

Abstract

The modern Bass Canyon is one of the world's largest submarine canyon systems that is entirely located within a cool-water carbonate environment. Five large shelf-breaching and three slope-confined tributary canyons coalesce on the lower slope and enter the massive deep-water Bass Canyon at 3000 m depth. Normal slope sediments consist predominantly of sandy calcilutite and muddy calcarenite interpreted as mud flow and mud-lubricated sandy debris flow deposits respectively, and hemipelagic foraminiferal calcilutite. Canyon head sediments consist of intraclast-rich calcarenite and calcirudite, probably deposited by mass-wasting events, and fine calcarenite, deposited by cohesionless sandy debris flows. Canyon filling sediments consist of well-sorted fine calcarenite deposited by (long term) semi-continuous cohesionless sandy debris flows, and rarer intraclast-rich mud, interpreted as cohesive sediment gravity flow deposits. Two types of tributary canyons are recognized: V-shaped canyons with steep walls (up to 35°) that are well-defined by backscatter acoustics; and broad U-shaped canyons (walls ≤ 10°) poorly defined by backscatter. It is most likely that tributary canyons developed from down-slope eroding sediment gravity flows triggered at the shelf break, which mature to develop dendritic canyon heads. Dendritic canyon heads entrain coarse-grained shelf sediment, which fuel erosive gravity flows and scour deep V-shaped canyon profiles. Once canyon heads stabilise, shelf-derived erosive sediment flows are reduced and the canyon profile switches from V- to U-shaped. This is aided by continual pelagic sedimentation and sediment gravity flows from the adjacent slope and canyon walls. Mud-free sandy debris flows from the lower slope converge with sandy outflows from tributary canyons and flow down the Bass Canyon floor. Sand cored from the Bass Canyon floor preserves cyclic fluctuations in magnetic susceptibility. High magnetic susceptibility zones are associated with increases in cool-temperature planktonic foraminiferal, and have been tentatively correlated to oxygen isotope stages 6.2–6.8 (135–185 ka) and 8.2–8.4 (245–278 ka). Based on this correlation, sedimentation rates on the slope and within the Bass Canyon were found to be highest during the highstand and regressive systems tracts, and lowest during the lowstand and transgressive systems tracts.
© 2006 Elsevier B.V. All rights reserved.

Keywords: submarine canyon; cool-water carbonate; sediment gravity flow; density current; headward erosion; sedimentation rate; magnetic susceptibility; oxygen isotope; sequence stratigraphy

1. Introduction

Submarine canyons are among the most significant features on continental margins the world-over. They act as important conduits delivering shallow water sediment to the deepwater environment, potentially creating

* Corresponding author.
E-mail address: j.mitchell8@pgrad.unimelb.edu.au (J.K. Mitchell).

0025-3227/$ - see front matter © 2006 Elsevier B.V. All rights reserved.
doi:10.1016/j.margeo.2006.10.037

significant hydrocarbon reservoirs and lithostratigraphic traps. The offshore Gippsland Basin is a cool-water carbonate system on the southeastern continental margin of Australia (Fig. 1) and hosts one of the world's largest submarine canyons — the Bass Canyon (Fig. 2). Recent high-resolution seabed mapping of the Gippsland Basin reveals a complex system of tributary canyons with a variety of morphologies. Comprehensive piston core and sediment surface sampling from the shelf to deep canyon floor provide the lithological data to develop a sediment facies model for the Bass Canyon system and further our understanding of canyon evolution.

1.1. Geological setting

The Gippsland Basin is the most eastern of Australia's southern continental margin basins, formed during the break up of eastern Gondwana in the Mesozoic and Cenozoic. It occupies an area of 56,000 km^2 of which, two thirds is presently offshore (Smith, 1982). Rifting and thermal subsidence allowed the deposition of Lower Cretaceous to Eocene fluviatile, lacustrine and marginal marine clastic sediment of the Strzelecki and Latrobe Group. Continued thermal subsidence during the Oligocene allowed the Tasman Sea to transgress over most of the basin, depositing up to 2500 m of fully marine carbonate-dominated sediment known as the Seaspray Group (Veevers, 1986; Rahmanian et al., 1990; Veevers et al., 1991; Willcox et al., 1992; Bernecker et al., 1997; Moore, 2002).

The Bass Canyon is an 80 km long, narrow (10 km wide) and linear, southeast trending flat bottomed canyon located at 3000–4000 m depth in the Gippsland Basin. Entering the head of the Bass Canyon at 3000 m depth are five shelf-breaching tributary canyons (Figs. 2–4) and three slope-confined tributary canyons. Although the age of the present-day canyon system is unknown, incisions across the modern shelf break date to the latest Pliocene (Mitchell et al., 2007). Buried canyon structures occur throughout the Seaspray Group from the late Oligocene but are particularly prevalent from the Middle Miocene to recent (Feary and Loutit, 1998).

1.2. Oceanographic setting

The offshore Gippsland Basin and Bass Canyon lie between 38 and 39 S. Mean sea surface temperatures vary from 12 to 20 °C annually, and the 15 and 10 °C isotherms occur approximately at 100 and 400 mbsl respectively (Levitas, 1982). The wind climate is dominated by westerlies (especially in winter) producing a moderate to high-energy wave-dominated environment and an eastward-moving winter-time current, which is forced from the west of Bass Strait by the Leeuwin and Zeehan currents, and by wind stress within Bass Strait (Li et al., 2005) (Fig. 1). This eastward movement produces a local winter phenomena called the Bass Cascade (Godfrey et al., 1980) where cold, dense and more saline water from the Bass Strait sinks below the warmer fresher water of the Tasman Sea just a few kilometres landward of the 200 m isobath. In summer, waters from the East Australia Current occasionally extend far enough south to reverse the movement of water in the Gippsland Basin (Li et al., 2005).

1.3. Previous work

The Bass Canyon and its largest tributary, the Everard Canyon, were first described by Conolly

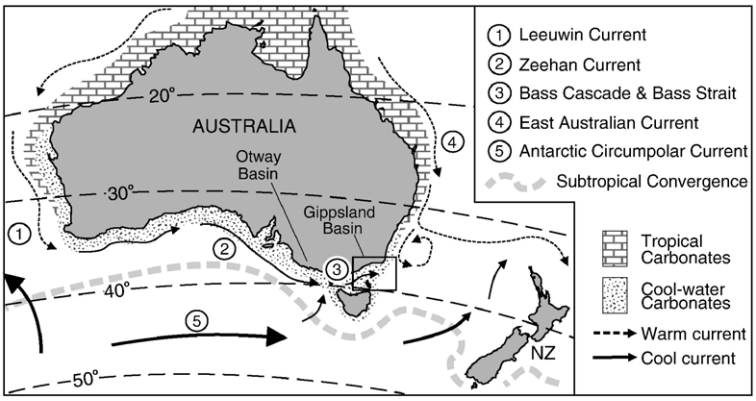

Fig. 1. Gippsland Basin locality and major geostrophic currents effecting the southern Australian margin. After Smith et al. (2001) adapted from Martinez (1994) and James et al. (1999).

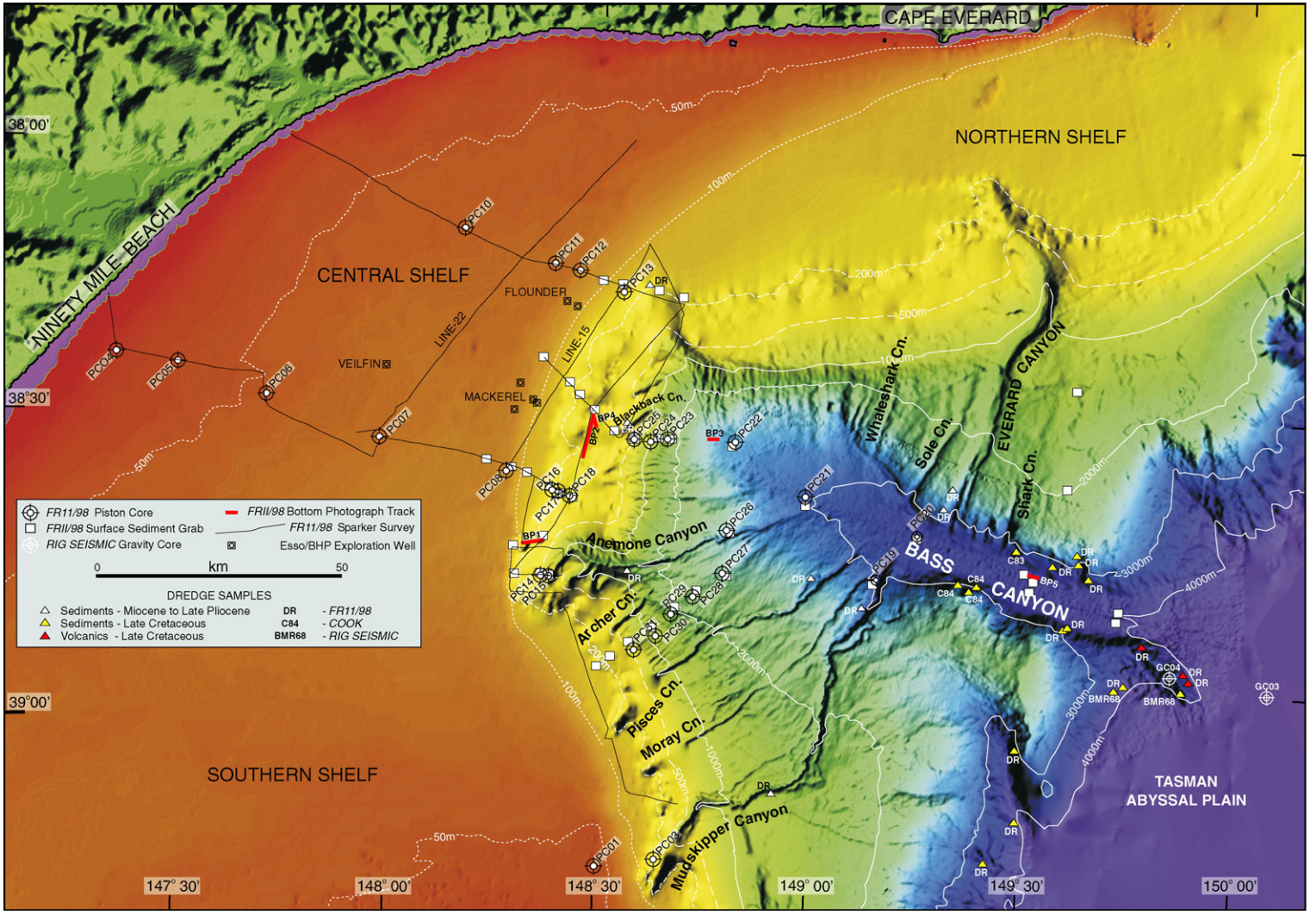

Fig. 2. High-resolution swath-map seafloor bathymetry image of the Offshore Gippsland Basin and Bass Canyon. Locality of data acquired during the *R/V Franklin* cruise (1998) and earlier cruises. Bathymetry data provided by *AGSO*/*GSA*.

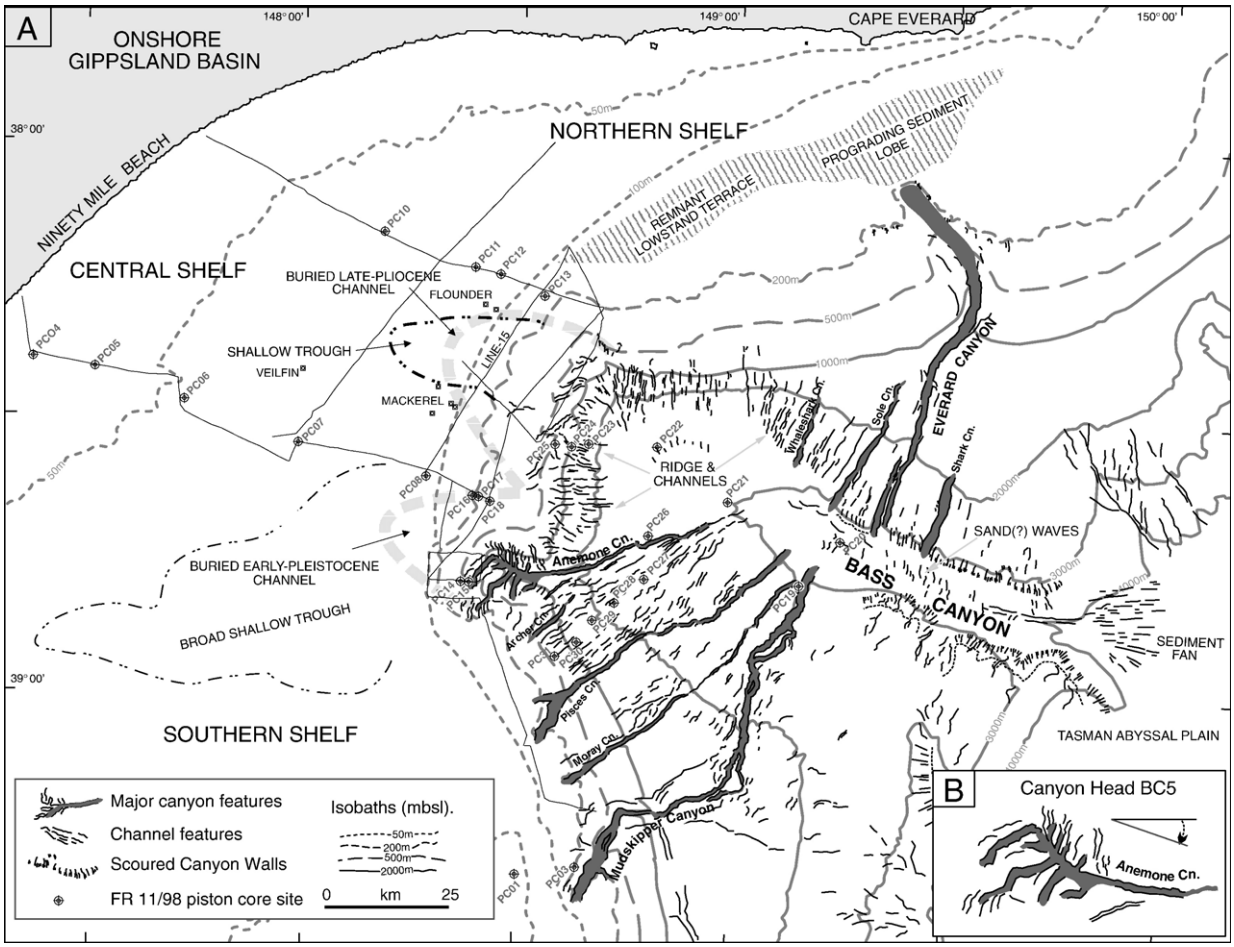

Fig. 3. A. Interpretation sketch of offshore Gippsland seafloor morphological features. Showing location of *R/V Franklin FR11/98* survey and piston core sites, along with approximate position of buried Pliocene and Pleistocene channels. B. An enlarged and rotated sketch of the asymmetrical canyon head of Anemone Canyon showing similarity of asymmetry to the Bass Canyon system. Both have deep V-shaped incisions on southern slopes and small, broad valleys on northern slopes.

(1968) using soundings from the Royal Australian Navy Hydrographic Office. A number of studies presented facies distribution maps for surficial sediments on the Gippsland shelf and Bass Strait (Davies and Marshall, 1973; Jones and Davies, 1983; Smith et al., 2001) and on the adjacent southern New South Wales continental margin (Davies, 1979). The first modern sediment samples collected from the Bass Canyon were reported by Schneider (1985) and Colwell et al. (1987) from a limited number of cores and dredges. The HMAS *Cook* cruise dredged Upper Cretaceous sediments from canyon walls (Marshall, 1988). Comprehensive sampling of recent sediments within the Bass Canyon system was not undertaken until the *RV Franklin* cruise in 1998 (*FR11/98*) (Exon et al., 2002; Smith and Gallagher, 2003) (Fig. 2).

The onshore Oligocene to recent sediments of the Gippsland Basin are well studied, whereas the offshore equivalents are less well understood. The only formal offshore subdivisions are those of Holdgate et al. (2000) which are: the deep-water Oligocene to Middle Miocene Angler Subgroup; the Middle Miocene to Late Miocene outer-shelf to upper slope, largely carbonate-rich canyon facies of the Albacore Subgroup; and of most interest to this study, the Pliocene to recent, predominantly carbonate-rich shelf and canyon facies of the Hapuku Subgroup.

To date, the most comprehensive study of Pliocene to recent sediments in the offshore Gippsland Basin is that of Holdgate et al. (2003) who concentrated on shelf sediments, analysing litho- and biostratigraphic samples from eight *Esso/BHP* oil and gas platform foundation

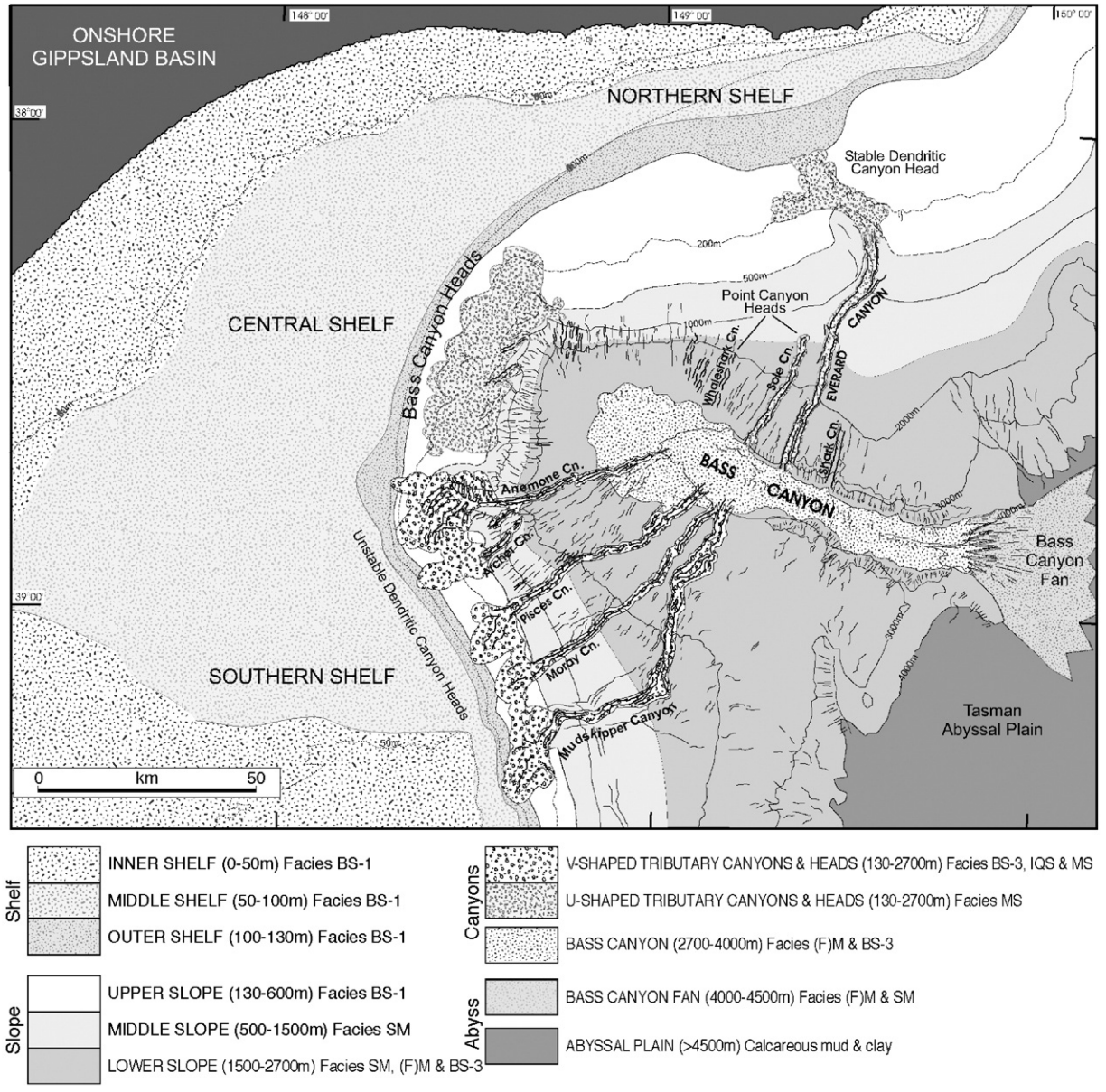

Fig. 4. Major sedimentary environments and predominant sediment facies of the offshore Gippsland Basin and Bass Canyon system.

bores, surface grab samples (after Smith et al., 2001), piston cores and a shallow seismic from the *FR11/98* cruise. In this study we established a biostratigraphic framework for the mostly carbonate Pliocene to recent shelf sediments, incorporating palynology (McMinn, 1992), calcareous nannofossils (Shafik, 2000) and foraminiferal studies (Mays, 2001; Gallagher et al., 2003; Holdgate et al., 2003). Sediments were assigned to a range of nanno-zones from the Early Pliocene nanno-zone CN10d-11 through to the Late Pleistocene to recent nanno-zone CN15.

1.4. Methodology

The *R/V Franklin* cruise of September 1998 (*FR11/98*) obtained 29 sediment piston cores (Keene, 1998) across the Gippsland shelf, slope, canyon heads and floor of the Bass Canyon in water depths from 35 m to 3344 m. The corer had a 300 kg weight stand and a 20 kg trigger weight. Sediment recovery ranged from 0.36 m to 5.20 m. All cores had a small amount of water above the sediment, suggesting that top-of-core loss was not an issue. All cores were logged for magnetic

susceptibility and sampled for texture, grain-size, calcium carbonate content, petrology and diagenetic microscopy. Eleven cores were previously studied by Holdgate et al. (2003) in their shelfal study, and 4 cores (PC06, 18, 21, 28) were assigned nannofossil zones by Shafik (2000) from base-of-core samples. In addition, 17 dredge samples and 72 sediment grabs were collected (Keene, 1998; Smith et al., 2001; Exon et al., 2002; Smith and Gallagher, 2003). Samples were complemented with lithological and palaeontological descriptions obtained during the HMAS *Cook* cruise (Marshall, 1988; Exon et al., 2002) and the *Rig Seismic* cruise (Colwell et al., 1987) (Fig. 2).

Forty samples across a variety of sediment facies were split into mud, sand and gravel size fractions by wet sieving across 62 μm and 2 mm sieves, and classified according to the *Folk* scheme. Sediment with less than 50% carbonate by weight are referred to as calcareous-mud, -sand and -gravel. Sediments with greater than 50% carbonate are referred to as calcilutite, calcarenite and calcirudite. More than 150 samples were analysed for carbonate content using the method of Wallace et al. (2002). Analytical precision was ±2% (SD=2.01 at n=35). Twenty four thin-sections were created from vacuum impregnated piston core samples. Grain-petrology percentages were approximated using visual comparison charts (Bacelle and Bosellini, 1965). High resolution seabed mapping and backscatter data of the southeastern Australian margin was produced and supplied by Geoscience Australia using multi-beam swath-mapping (Simrad EM1002) technology (Exon et al., 1999; Harris et al., 2000). Airborne magnetic imagery of the Gippsland Basin was supplied by the Geological Survey of Victoria (Fig. 18). In addition, seafloor bottom photographs were taken during the *FR11/98* cruise (Keene, 1998) (Fig. 15).

2. Seafloor morphology and sedimentary environments

This study divides the offshore Gippsland Basin marine geology into shelf (inner, middle and outer); slope (upper, middle and lower); canyons (canyon heads, tributary canyons and the Bass Canyon); and the Tasman Abyssal Plain (Fig. 4). The following sections describe the physical characteristics of the major sedimentary environments.

2.1. Shelf (0–130 m water depth)

The present day Gippsland shelf has a gently dipping (0.08°) planar surface that extends seaward from the

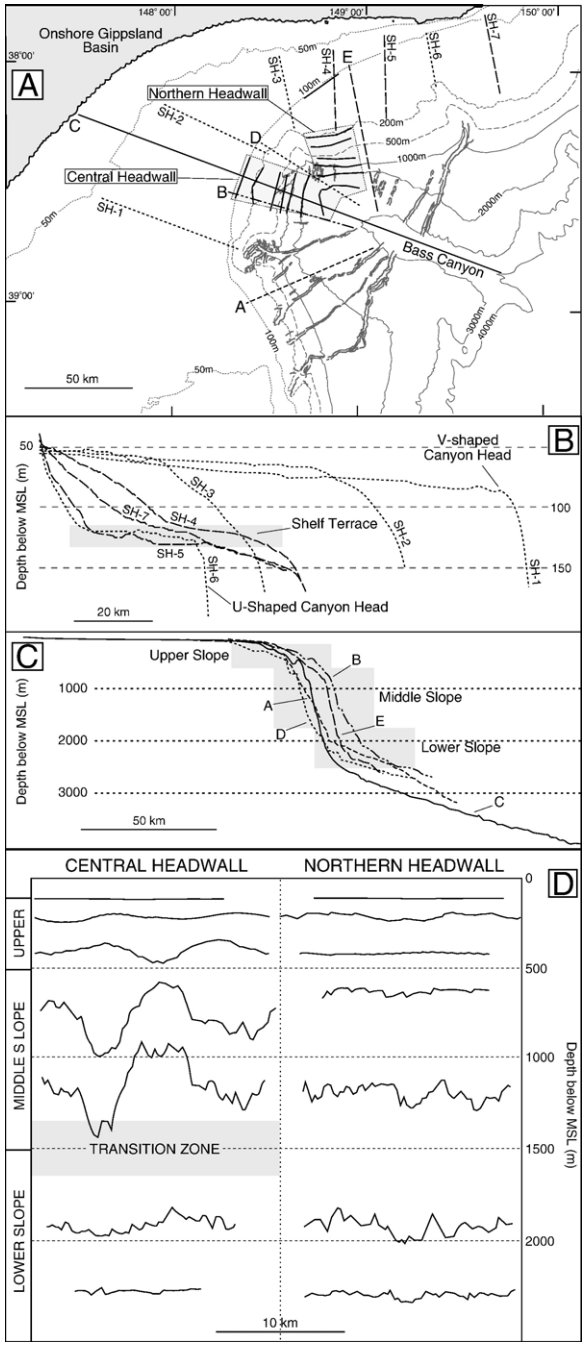

Fig. 5. A. Locality of shelf and slope profiles. B. Shelf profiles. SH-4 to SH-7 all preserve a terrace at 120–130 m water depth. Profiles SH-1,2,3 and 6 all intercept canyon head environments at the shelf break. C. Shelf to Slope profiles showing upper-, middle- and lower slope changes in gradient. D. Profiles of traverses across the central headwall/slope (left) have large channels on the upper and middle slope that relate to canyon heads. These channels are overprinted by 'ridge and channel' features in the middle and lower slope. The Northern headwall/slope (right) is free of canyon head systems and 'ridge and channel' features are predominant from the base of the upper slope to the lower slope.

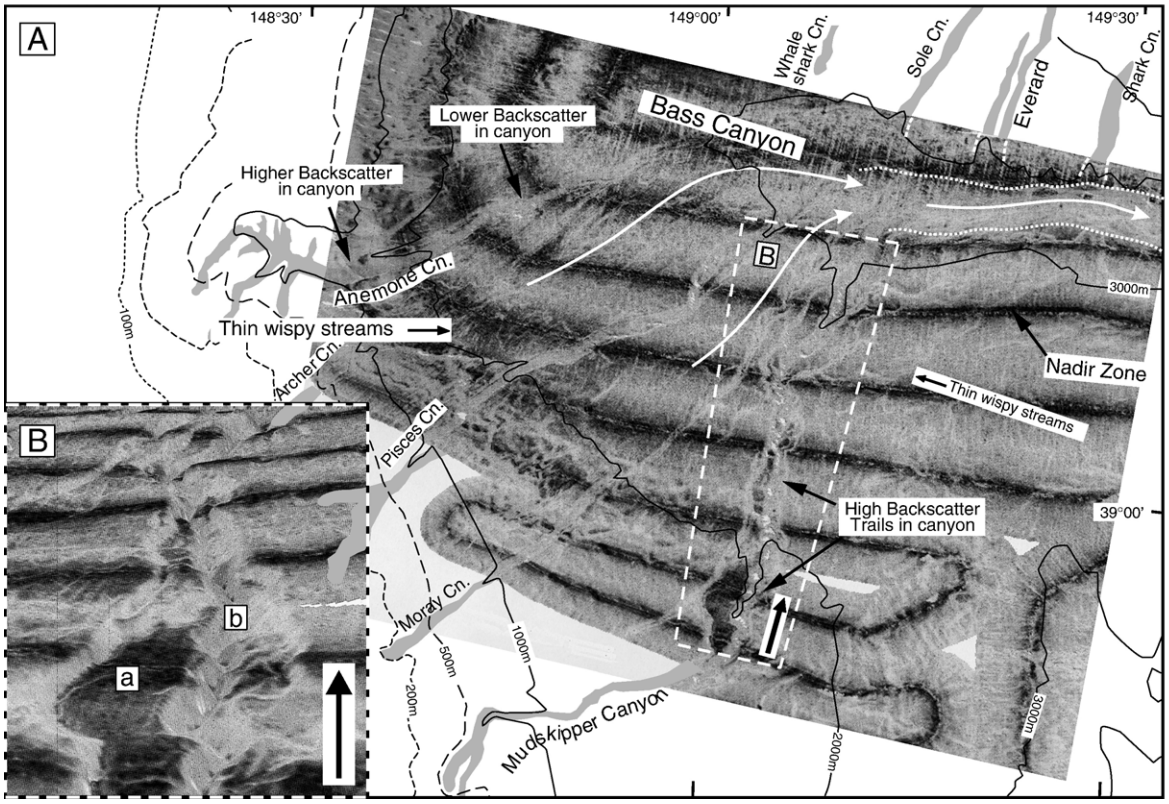

Fig. 6. A. Seafloor backscatter image of the Bass Canyon system. Low backscatter surfaces are white and high backscatter surfaces are black. High backscatter regions include some canyon surfaces and sediment trails within canyon floors. Low backscatter regions include wispy stream-like features on the slope interpreted as mud flows. Strangely, many areas within canyons also produce low backscatter. Down-slope sediment transport flow paths are clearly visible and show low-backscatter sediment streams converging at, and funnelling down, the Bass Canyon. B. 3D Backscatter image looking north down Mudskipper Canyon (a) High backscatter surface of a raised island within the main channel of Mudskipper Canyon, which may represent a large mass-wasting deposit. (b) Relatively low backscatter within canyon floor may indicate the presence of a thin mud veneer or very smooth silt to fine sand substrate.

coastline to an average depth of 130 m (110–150 m range). The shelf is 40 km wide south of Cape Everard and broadens to 120 km west of Ninety Mile Beach (Figs. 2–4). To the southwest the shelf extends 450 km across the shallow shelf that forms Bass Strait. Shelf subdivisions have been arbitrarily based on water depths (Inner 0–50 m, Middle 50–100 m, and Outer 100–130 m).

At 110–130 m depth along the northern shelf is a 10–16 km wide terrace (Figs. 3 and 5B), which extends (at the eastern end) to the head of the Everard Canyon. On the central shelf, east of the Veilfin Platform, a very broad shallow trough trends east between the Mackerel and Flounder platforms to where it is best developed below shallow seismic line L15 (Fig. 3). Here it is 20 km wide and 30 m below the level of the adjacent central shelf. Further to the east the trough merges into the headwall of the Bass Canyon at about 200 m water depth (Fig. 3). A second much broader shallower trough or depression is located to the south of the central shelf and opens around the head of the Anemone Canyon. At its widest this trough is 50 km across and 25 m below the adjacent shelf. Both of these troughs overlie buried Plio/Pleistocene channels (Mitchell et al., 2007). With the exception of these features and the near-shore zone, the remainder of the shelf is uniformly planar at the resolution of the data.

2.2. Slope (Upper 130–600 m, Middle 600–2000 m, Lower 2000–3000 m water depth)

The shelf break marks a relatively well-defined transition from the very shallow-dipping shelf to more steeply dipping seafloor, at approximately 130 m water depth (Figs. 4 and 5C). In general, the upper slope extends seaward for approximately 30 km at an average of 1.1° then abruptly steepens to 4.5° at the middle slope near 600 m depth (range of 340–800 m). Where the

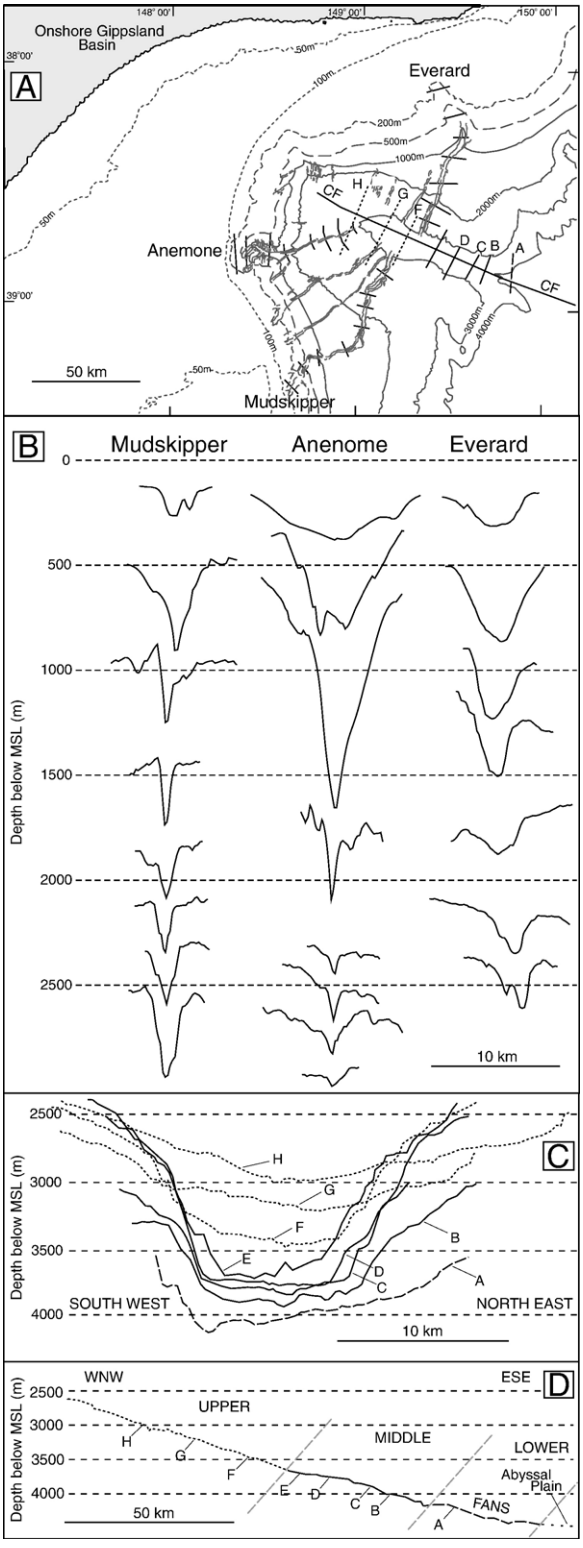

gradient steepens to 4°, parallel and linear, V-shaped ridge and channel features have developed and run down slope (Figs. 2 and 3). Channel dimensions vary from 500–3500 m in width and 50–170 m in depth, but rarely exceed a depth to width ratio of 0.1 (Fig. 5D — Northern Headwall). They are best developed at water depths of 1000–2200 m and are largest when dendritic canyon heads are absent up slope. Similar features on 3D seismic have been referred to as slope-confined canyons by Bertoni and Cartwright (2005) or 'pre-canyon rills' by Pratson and Coakley (1996). On slopes with lower gradients, ridge and channel features are absent. Present instead, are thin, sinuous stream-like features visible as low backscatter wisps (Fig. 6).

Across the basin, the middle- and lower slope maintain a fairly constant gradient down to 2500 m depth before flattening to 2.5° towards the Bass Canyon (Figs. 2–4 and 5C). The boundary between the middle- and lower slope is approximately defined at 1750 m depth. This is based largely on a sedimentary facies change, marked by a significant increase in the proportion of sharp-based sandy units in relation to massive mud units (Sections 3.2 and 3.3 below).

The prominent ridge and channel features of the middle slope rapidly flatten and disappear below 2200 m as the gradient of the slope approaches that of the Bass Canyon floor. In this region, thin, stream-like, low backscatter zones converge towards and enter the Bass Canyon (Fig. 6). Outside of the Bass Canyon system, the base of the slope intercepts the Tasman Abyssal Plain at about 4000 m (Figs. 2 and 4). Because the continental margin is strongly embayed around the deep-water Bass Canyon, a continental rise is not defined here.

2.3. Canyons

Submarine canyon environments within the Gippsland Basin can be subdivided into tributary canyons, canyon heads and the Bass Canyon:

- *Tributary canyons* are defined as channel-like features that extend in length for greater than 10 km, while maintaining a minimum trough to

Fig. 7. A. Locality of profiles across some of the major tributary canyons of the Bass Canyon system and the Bass Canyon. B. Cross-channel profiles of Anemone and Mudskipper canyons (V-shaped) and the Everard Canyon (U-shaped). C. Profiles A–H run normal to the central Bass Canyon axis. D. An axial profile of the Bass Canyon. The floor has been divided into three sections based on morphology. Lower (A) consists of fans; Middle (B–E) narrow, linear and flat bottomed; Upper (F–H) is broad and open.

shoulder height of 150 m, and feed directly into a larger canyon system.

- *Canyon heads* are the upslope limits of canyons. Two types are recognised; *dendritic* canyon heads that develop on the shelf break, and non-dendritic canyon heads associated with slope-confined canyons. We suggest the term *point* canyon head may be used for non-dendritic canyon heads.
- The *Bass Canyon* is the 80 km long, linear, southeast trending canyon located at 3000–4000 m depth (Figs. 2–4).

2.3.1. Tributary canyons (150–3500 m water depth)

The Bass Canyon system has five major tributary canyons that breach the shelf and extend farther than 40 km down slope to their point of capture within the Bass Canyon at depths of greater than 3000 m. Each major tributary canyon alone is large in comparison to the United States Atlantic canyons, such as the Baltimore and Hudson canyons (Twichell and David, 1982; Farre et al., 1983; Pratson et al., 1994; Pratson and Coakley, 1996). Four of the five major tributaries occur on the southern slopes (Anemone, Pisces, Moray and Mudskipper) and one, the Everard Canyon, occurs on the northern slopes (Figs. 2–4). In addition, there is one shelf-breaching canyon that terminates at the middle/lower slope boundary on the southern slope (Archer Canyon) and three slope-confined canyons that intercept the Bass Canyon on the northern slope (Shark, Sole and Whaleshark canyons). No tributary canyons are found on the slope beneath the central shelf. However, there are a number of broad channels present here on the shelf break, the biggest of which, has been referred to as the Blackback Canyon by *Esso* engineers (Henry et al., 2000). Initially these channels trend northeast across the shelf break before running normal to the slope below the 200 m isobath (Figs. 2 and 3). They are typically 5–10 km wide and cut 60 m deep increasing to 300 m near the upper/middle slope boundary (Fig. 5D — central headwall and slope). Channel walls become progressively steeper with depth, reaching a maximum of 10°. Upper slope channel morphology is overprinted by higher-frequency, linear, V-shaped ridge and channel systems on the middle slope (Fig. 5D).

All tributary canyons on the southern slope have narrow, V-shaped profiles, while all canyons on the northern slope have U-shaped profiles. V-shaped tributaries maintain narrow profiles throughout their entire course, with typical channel depth to width ratios of 0.15. The walls of V-shaped canyons may approach gradients of 35°. In comparison, U-shaped canyons are broad and produce depth to width ratios of less than 0.09 (Fig. 7B) with walls rarely exceeding gradients of 10°. Backscatter data reveal that all V-shaped canyons are well-defined with generally slightly lower backscatter properties than their adjacent slope sediments, but include isolated regions and trails of very high backscatter within canyon floors (Fig. 6). U-shaped canyons are not defined by backscatter properties, although, the data only covers the lower limits of these canyons. Low backscatter properties within canyons are unusual as canyons are normally associated with higher backscatter responses (Kenyon et al., 2002; Hill et al., 2005), discussed in Section 4.6.

Slope gradient appears to control the thalweg of the tributary canyons. At gradients of 2° or higher channels are linear and do not bifurcate. At 1.8° or less canyons may begin to meander, and at lower gradients my bifurcate or braid. Additionally, V- and U-shaped tributaries are spaced relatively evenly across the slope at 11 km±3 km intervals, discussed in Section 4.2.

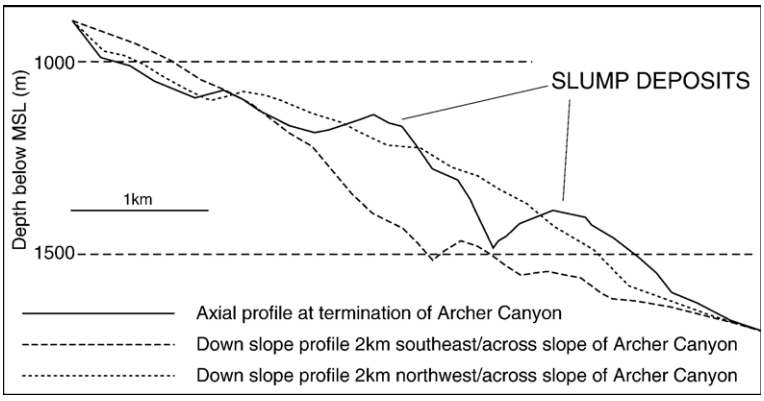

Fig. 8. Profiles of the down-slope terminus of Archer Canyon. The main axial profile identifies two morphological features that resemble large slump deposits. Profiles taken on the adjacent slope (2 km either side) have relatively smooth bathymetry.

Table 1

Facies	Lithology	$CaCO_3$%	% of cored sed. & sediment relationships	Bedding & sediment structures	Texture & sorting	Grain/lithoclast composition	Depositional process	Environment of deposition
BS-1	Grey-orange quartzose bioclastic calcarenite — Grainstone & Floatstone	25–85%	(18%) —Interbedded with (M)G & IQS.	Sharp erosional bases, massive or normally graded, submetre-thick bedding.	Mud-free, moderately well-sorted, medium to coarse sand.	Bivalves, bryozoans, quartz, echinoids, gastropods, red algae	Wave graded.	Inner to outer-shelf.
(M)G	Grey-orange molluscan shell bed — Rudstone	45–75%	(6%) —Interbedded with BS-1.	Often sharp-based, with decimetre-thick planar beds.	Poor to very-poorly-sorted and skeletal supported, valves generally concave-up.	Bivalves, bryozoans, gastropods in a quartzose calcarenite matrix.	Near-*situm* shell bed; low to mod.–energy wave graded.	Inner to middle shelf
(BM) MS	Light green-grey bryozoan–molluscan muddy calcarenite — Floatstone	60–65%	(2%) — Gradational below with SM. sharply overlain by MS.	Massive, decimetre-thick bedding with gradational (bioturbated) contacts.	Very poorly-sorted, gravel-sized to fine sand-sized bioclasts within a calcareous mud matrix. Bioturbated.	Bryozoans, bivalves, gastropods, echinoids & calcareous worm tubes, with silt to fine sand sized quartz.	Hemipelagic settling and in-*situ* carbonate production.	Upper slope
MS	Medium green-grey muddy fine-grained calcarenite — Packstone & Wackestone	55–80%	(22%) — Primarily gradational with SM. Sporadically interbedded with BS-2.	Usually massive, often reverse graded, rarely normally-graded, metre-scale bedding. Contacts sharp & planar or gradational, rarely erosional.	Generally grain-supported. Poor to moderately-sorted. Often weakly laminated.	Med.-coarse sand-sized bioclasts (mollusc/forams/ bryozoan), fine quartz sand, pelloids & organic fragments common. Rare mud clasts. Organic-rich calc. mud matrix common.	Sandy debris flow–mud-lubricated.	Upper to middle slope. Occasionally on lower slope.
SM	Light green-grey sandy calcilutite — Wackestone	60–75%	(26%) — Gradational with MS & (BM)MS. Sporadically interbedded with BS-2 & BS-3.	Metre-scale bedding, massive or reverse graded, rarely normally-graded. Contacts gradational or occasionally planar. Rare cm-long sand-filled burrows.	Very poorly-sorted, matrix-supported.	Sand-sized shelf-derived bioclasts, plank.forams. and qtz silt in a calcareous clay-rich matrix.	Cohesive debris flow–mud flow.	Middle & lower slope. Occasionally Upper slope & canyon

								floor
BS-2	Light green-grey quartzose bioclastic calcarenite — Packstone	60–80%	(2%) — Interbedded with MS & SM.	Sharp planar lower contacts, massive or normally-graded, thin (>0.10 m) thick beds. Upper contacts sharp or rapidly gradational.	Mod. to poorly-sorted, muddy, grain-supported, fine to med.-grained sand.	Bioclasts of well worn mollusc, bryozoan, & foraminifera very common, with quartz sand.	Mud-lubricated sandy debris flow.	Upper-slope & canyon heads
BS-3	Light grey-green to brown-grey quartzose bioclastic calcarenite — Grainstone	45–80%	(16%) — Sharply overlies MS, SM, (F)M & locally over IQS.	Sharp planar or erosional bases, normally-graded, rarely laminated, sharp upper contacts. 0.30–3.5 m thick.	Very well-sorted, mud-free, grain-supported, fine sand to gravelly coarse-granular sand, with occasional lithoclasts & mud rip-up clasts.	Bioclasts of well worn mollusc, bryozoan, forams, echinoids, red algae and organic fragments, with quartz sand.	Cohesionless sandy debris flow or turbidity current.	Middle to lower slope & canyon floor
IQS	Dark grey intraclastic quartzose calcarenite — Floatstone & Rudstone	70–80%	(3%) —Overlain by or interbedded with BS-2.	Massive to normally-graded. Erosional lower contacts, sharp upper contacts.	Very poorly-sorted & matrix-supported. Med. to coarse, qtz-calcarenite matrix.	Rounded and angular, weakly-cemented bioclastic intraclasts, & worn & stained mollusc shell fragments.	Cohesionless sandy debris flow.	Steep upper canyon heads & tributary canyons
IMS	Medium green-grey Intraclastic Muddy Calcarenite — Floatstone	50–75%	(3%) —Interbedded with SM & BS-2.	Massive. erosional basal contacts, sharp upper contacts.	Very poorly-sorted, matrix-supported. Mud-rich fine-grained calcarenite matrix.	Rounded to angular weakly-cemented bioclastic intraclasts & mud clasts. Mollusc & bryozoan fragments, qtz sand & organic fragments.	Cohesive debris flow.	Confined channels; tributary canyon
(F)M	Green-grey-brown foraminiferal calcilutite — Mudstone & Wackestone	60–65%	(2%) — Truncated by BS-3.	Sharp or gradational lower contacts, massive.	Very poorly-sorted and matrix-supported. Often organic-rich, calcareous, clay-rich matrix.	Planktonic foram. tests, silt to fine sand-sized quartz, silt-sized organic fragments & fine sand-sized shelf-derived bioclasts.	Hemipelagic settling.	Lower slope & canyon floor

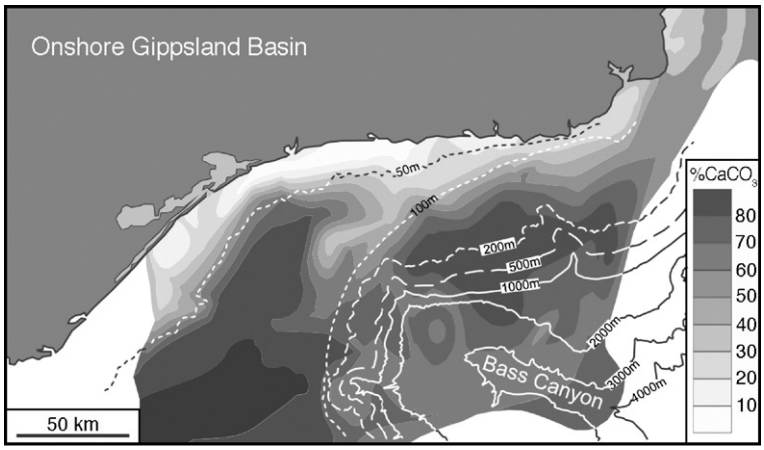

Fig. 9. Carbonate contour map of sediments on the offshore Gippsland Basin seafloor after Smith et al. (2001) adapted from Holdgate et al. (2003).

The short shelf-breaching Archer Canyon (Fig. 2) maintains a narrow V-shaped incision throughout, but is terminated near the middle/lower slope boundary by two 50–100 m high slump-like structures (Fig. 8). Conversely, the slope-confined U-shaped canyons on the northern slopes (Shark, Sole and Whaleshark, Fig. 2) feed into the Bass Canyon, but dissipate above on the middle slope to a point canyon head.

2.3.2. Canyon heads (130–500 m water depth)

Dendritic canyon heads are associated with shelf-breaching canyons. In general, dendritic canyon heads

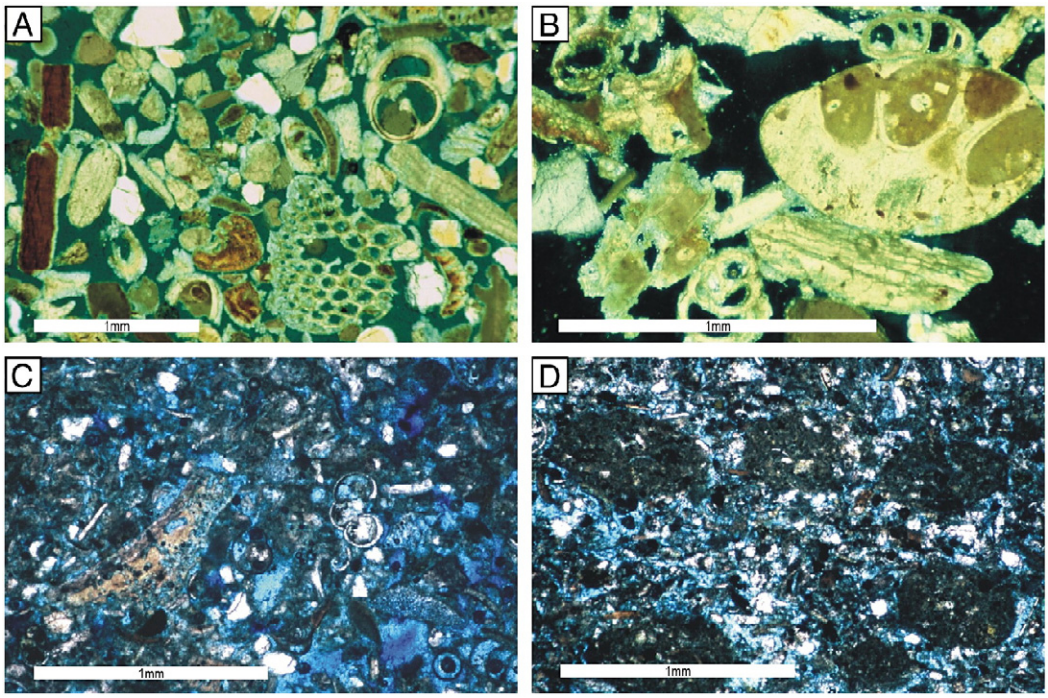

Fig. 10. Photomicrographs of resin impregnated thin-sectioned piston core. Resin is blue. A. (X-polar.) Facies BS-1 (PC08, − 0.25 m) typical of the inner and middle shelf. Grains are largely rounded, with abundant microbial boring and limonite staining. B. (X-polar.) Facies BS-1 (PC13, −2.50 m) incipient meniscus calcite cement present at many grain contacts and within intra-grain pores. Micrite cements present within some bioclasts. C. (Norm-polar.) Facies MS (PC25, −0.28 m) typical of the upper slope, with mixed shelf-derived bioclasts, hemipelagic mud and minor planktonic foraminifera. D. (Norm-polar.) Facies MS (PC30, −2.82 m) fine-grained peloid-rich muddy quartzose calcarenite typical of the middle slope.

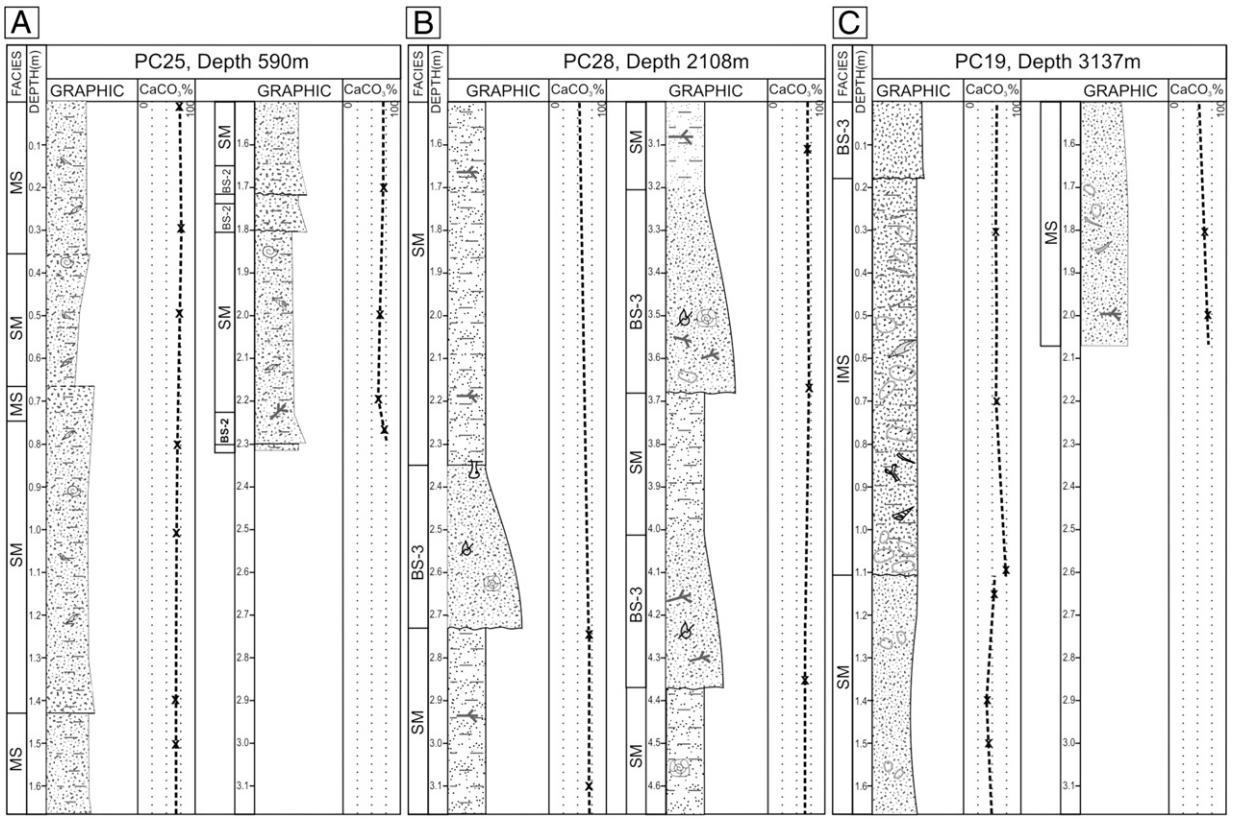

Fig. 11. A. Graphic log of piston core PC25 (590 m depth). Sharp-based, normal and reverse graded Facies SM, MS, and minor BS-2, typical of the upper slope. B. Graphic log of piston core PC28 (2108 m depth). Sharp-based, normally-graded Facies BS-3 interbedded with Facies SM, typical of the lower slope. C. Graphic log of PC19 (3137 m depth). Sharply bound Facies IMS interbedded with Facies SM, MS and BS-3 from lower region of Moray Canyon.

are comprised of closely-spaced steep-sided channels that branch upslope and appear to incise back into the shelf. Branches extend away from the central canyon axis at angles of 65°±15° producing a 'pinnate' form (Farre et al., 1983). The best example of this is observed at the head of the large Anemone Canyon (Figs. 2 and 3). The large U-shaped Everard Canyon on the northern slope also has a dendritic canyon head, although, its relief is very much lower than those associated with V-shaped canyons and appears to be filled-in. Within dendritic canyon heads, channels broaden above the 250 m isobath and adopt a smooth U-shaped morphology. Bottom photographs from this region within the Anemone Canyon reveal rippled sandy substrates, indicating the presence of traction currents (Fig. 15A).

The Anemone Canyon head is strongly asymmetrical and shares a similar symmetry to the Bass Canyon system. Channels on the northern wall are generally only 50–100 m deep and rarely exceed gradients of 10° while channels on the southern wall often incise 600 m deep with walls obtaining gradients of 35° or greater. In comparison, the southern slope of the Bass Canyon system has numerous deeply incised tributary canyons, while the northern slope has fewer less-incised tributaries, suggesting a regional canyon driving process (Fig. 3).

Point canyon heads are the upslope terminations of canyons that appear to have been buried in a downslope direction. They are only associated with slope-confined U-shaped tributary canyons, such as the Whaleshark, Sole and Shark canyons located on the northern slope (Figs. 2–4) and do not branch up slope.

2.3.3. Bass Canyon (3000–4000 m water depth)

The Bass Canyon can be divided into two sections based on morphology, plus a fan complex (Figs. 2–4 and 7C,D). The western, or upper, 45 km is steepest with an average gradient of 1° and incorporates the slope to floor transition. This section is up to 35 km wide

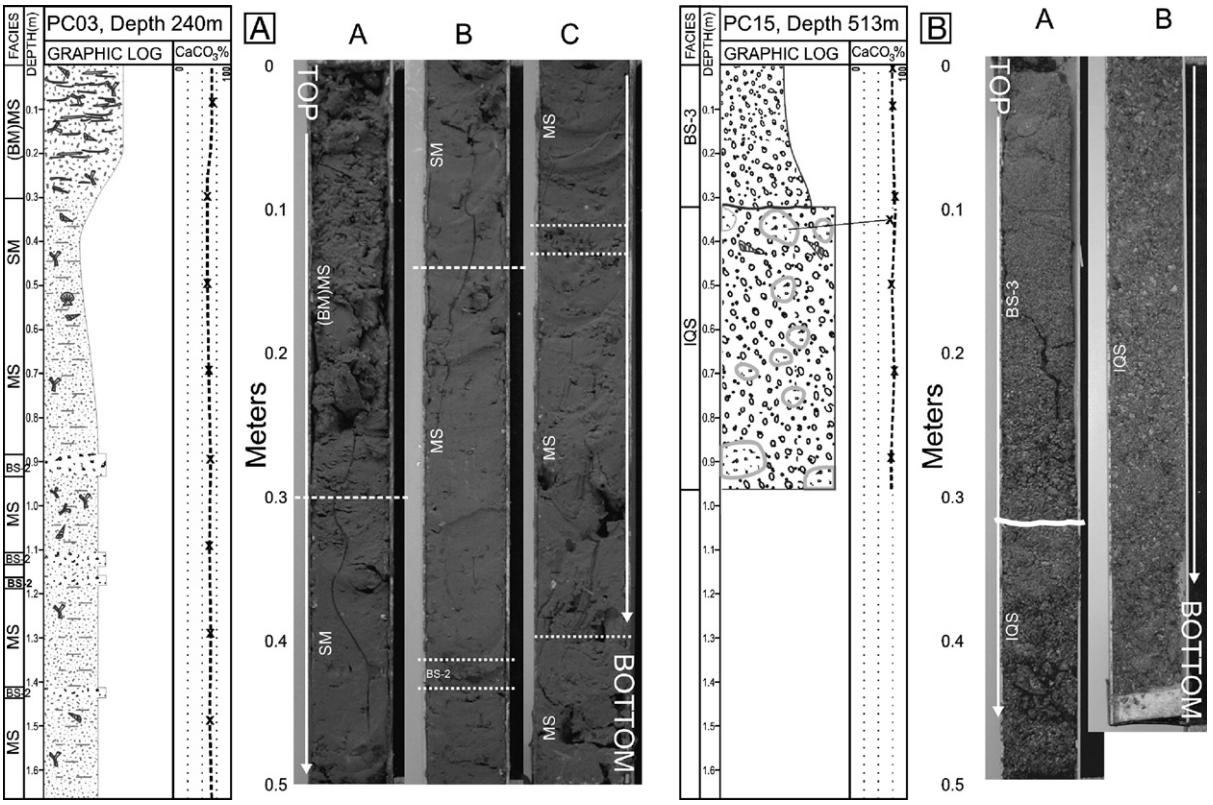

Fig. 12. A. Graphic log and photo of piston core PC03 (240 m depth). Facies (BM)MS, MS, SM and BS-2 from the upper slope and canyon head environment of Mudskipper Canyon. B. Graphic log and photo of piston core PC15 (513 m depth). Facies IQS and BS-3 from within the actively eroding steep V-shaped canyon head of Anemone Canyon.

and is the point of capture for the tributary canyons (Fig. 7C,D —profiles F–H). The lower section of the Bass Canyon is a 35 km long, narrow and straight-sided channel, which in cross-section has a near flat floor and sharp transitions to steep canyon walls (Fig. 7C,D—profiles B–E). Here the floor ranges in width from 6–10 km, with an average gradient of 0.8°. In this region of the canyon, walls approach gradients of 20°. Bathymetric data across the middle section of the canyon reveal subtle low-amplitude ridges that run perpendicular to the axis of the channel floor at approximately 1 km spacing (Figs. 2–4). Backscatter data reveal a concentration of low backscatter stream-like features that meander down the axis of the canyon floor fed from the southern slope tributary canyons (Fig. 6). Bottom photographs from a single traverse show a muddy, bioturbated surface, confirmed by multiple surface sediment grabs (Figs. 2 and 15B).

The mouth of the Bass Canyon ends in a fan complex that consists of three vertically stacked fans. The upper fan is smallest, and underlying fans are broader reaching 30 km across ((Figs. 2, 3 and 7)D — profile A). The surface of the fan complex undulates and has subtle radial lineations that extend from within the Bass Canyon to its outer edges. The abyssal plain immediately beyond this fan has a gradient of 0.3° or less and although, only partly imaged by swath-mapping, appears featureless.

3. Sedimentology of near-surface samples

The sediments analysed from the *FR11/98* piston cores have been divided into ten lithofacies based on texture, composition and sediment structures. The characteristics of each facies and their interpreted depositional process are detailed in Table 1. Core photographs, graphic logs, thin-section and seafloor bottom photographs of selected facies are shown in Figs. 10–16.

3.1. Bioclastic calcarenite-1 (BS-1) and Molluscan Shell Bed ((M)G)

Facies BS-1 is a grey-orange, moderately well−sorted sand composed of mollusc, bryozoan and foraminiferal

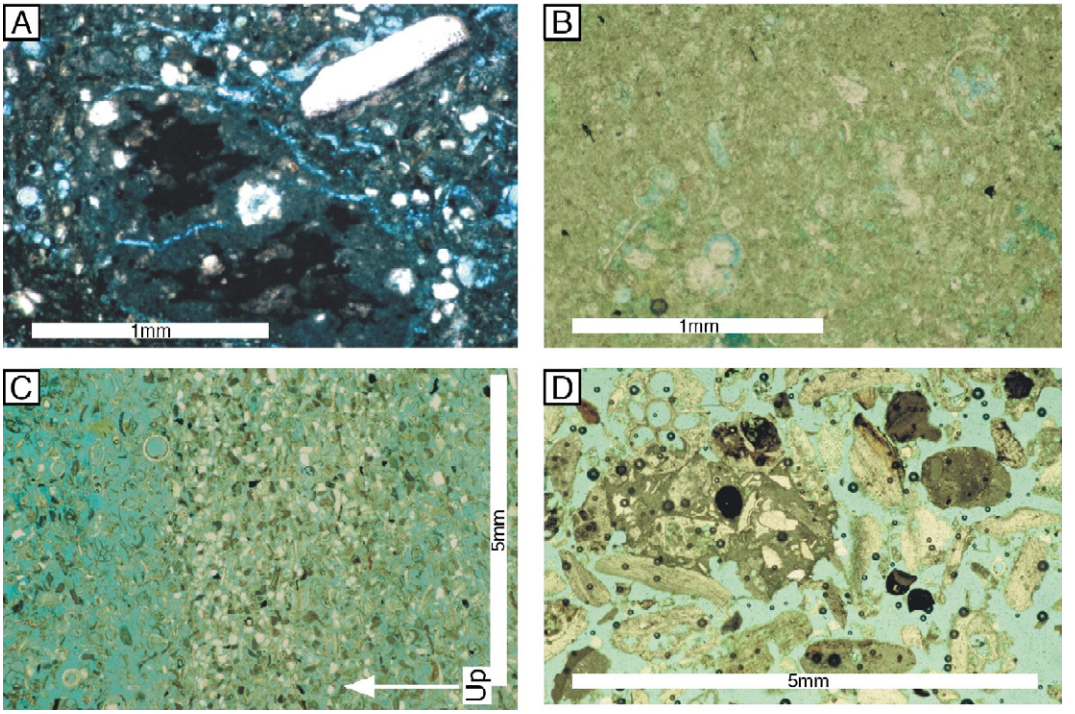

Fig. 13. Photomicrographs of resin impregnated thin-sectioned piston core. Resin is blue. A. (Norm-polar.) Facies SM/IMS (PC19, −1.73 m) matrix-supported, quartzose, bioclastic sandy calcilutite with abundant rounded mud rip-up clasts. B. (Norm-polar.) Facies (F)M (PC20, −3.60 m) slightly sandy, planktonic-foraminiferal calcilutite typical of lower slope and Bass Canyon floor. C. (Norm-polar.) Facies BS-3 (PC20, −0.35 m) laminated, very well-sorted, medium-fine calcarenite, cored from 3344 m depth in Bass Canyon floor. D. (Norm-polar.) Facies BS-3/IQS (PC14, −0.45 m) intraclast-rich coarse-grained bioclastic calcarenite from steep V-shaped Anemone Canyon head.

bioclasts with quartz (Table 1, Fig. 10A,B) and commonly alternates (on inner- and middle-shelf only) with decimetre-thick shell beds (Facies (M)G). Shell beds consist predominantly of large, thick-walled, well preserved, disarticulated bivalves generally deposited concave-up. The carbonate composition of facies BS-1 range from 7% at the coastal margins to 86% on the outer-shelf (Smith et al., 2001) (Fig. 9). Both facies were deposited within the influence of wave base.

The rounded, limonite stained and bored nature of bioclasts indicates that grains have been frequently remobilised and agitated and have had long residence times near the sediment surface before burial. The abundance of concave-up oriented valves ((M)G) indicates the absence of significant traction currents. Facies BS-1 is equivalent in part to the *quartz/carbonate sand/shell gravel* facies of Davies and Marshall (1973) and is interpreted by Jones and Davies (1983) as a mixture of Holocene transgressive and relict sediments. Facies (M)G is equivalent in part to the *quartz/carbonate sand/shell gravel* facies of Davies and Marshall (1973).

3.2. Muddy calcarenite (MS) and sandy calcilutite (SM)

Facies MS and SM are the predominant sediments on the slope (Table 1, Figs. 10C,D, 11, 12A, 13A). Both facies are poorly-sorted containing sand- and silt-sized bioclasts, silt-sized quartz and siliciclastic clay. Bioclasts commonly include shelf-restricted faunas, such as echinoderms and red algae, and have microbial boring and limonite staining. Many samples show subtle (sometimes distorted) laminations and weak grain-alignment in thin-section. Random rip-up clasts are common. Bioturbation is very rare. In general, pelagic mud and planktonic foraminifera increase with depth of deposition. Many units have sharp bases and are often reverse — as well as normally-graded.

Facies MS and SM may be similar to sediment facies described by Passlow (1997) from the adjacent Otway Basin, where deposition was attributed to the mixing of shelf and pelagic particles during remobilisation in downslope low-energy sediment gravity flows. Specifically, facies SM may be similar to both Facies-2 and Facies-3 of Passlow (1997), which are interpreted as mud flow deposits (or creeps). Facies MS may be

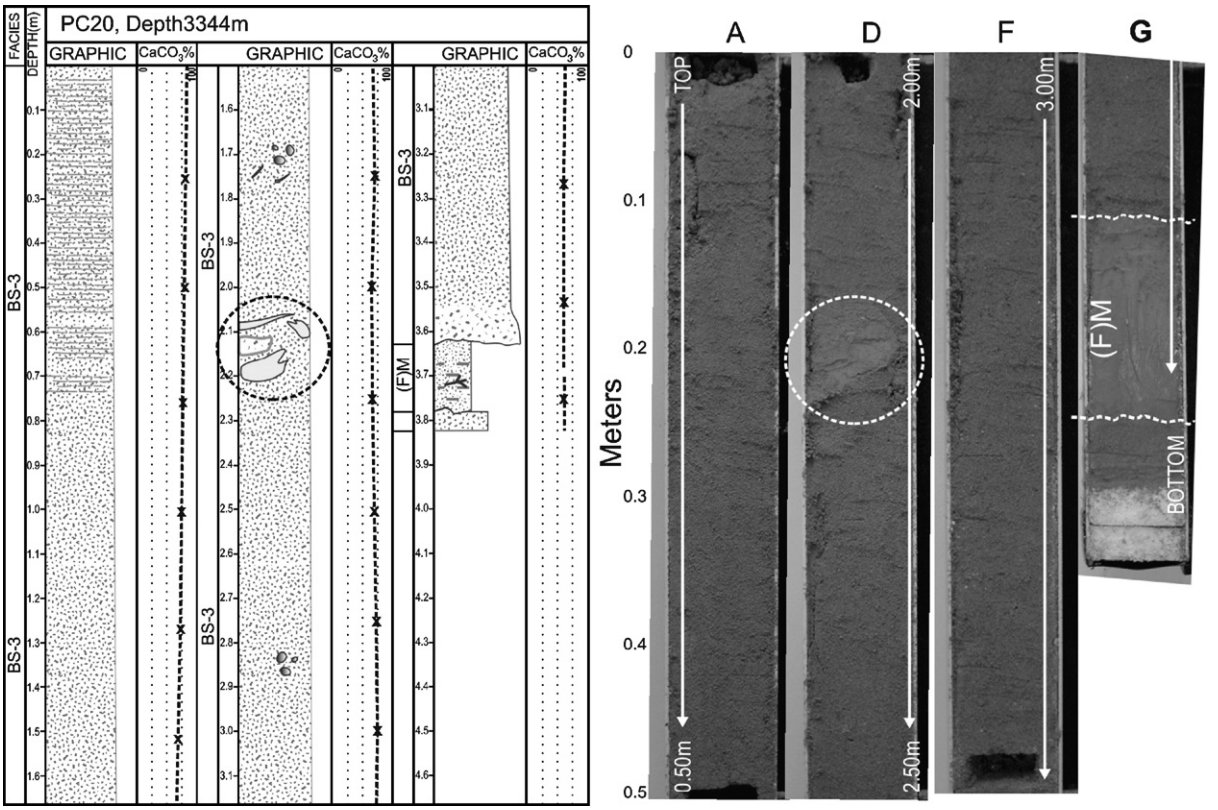

Fig. 14. Graphic log and photo of selected sections of piston core PC20. Facies (F)M overlain by 3.60 m of subtly normally-graded Facies BS-3. Cored from Bass Canyon floor at 3344 m depth.

similar to, but slightly coarser than, Facies-2 sediments of Passlow (1997) and are interpreted as mud-lubricated, sandy debris flow deposits.

3.3. Bioclastic calcarenite (BS-2) and (BS-3)

Both facies BS-2 and BS-3 are sharp-based, often normally-graded, quartzose, bioclastic calcarenites. BS-2 is mud-rich, poorly-sorted and generally has an abundance of planktonic foraminifera (Table 1, Figs. 11A and 12A). BS-2 forms centimetre-thick beds between facies MS and SM on the upper- and middle slope. BS-3 is mud-free, well-sorted and often coarse-grained. Bioclasts are well-rounded, commonly limonite stained, microbially bored and shelf-restricted species are often recognisable (Table 1, Figs. 11B,C, 12B, 13C and 14). BS-3 has been cored from the steep head of the Anemone Canyon and throughout the lower slope, and on the Bass Canyon floor, where it accounts for 97% of cored sediment (PC20–21). Within steep canyon heads, BS-3 is generally bound by intraclastic sand. On the slope it is bound by facies SM and MS, and on the Bass Canyon floor it is bound with pelagic mud.

BS-2 is similar to Facies-1 of Passlow (1997) and is likely to be deposited by small mud-lubricated sandy debris flows that haven't traveled far. Facies BS-3 sediments are interpreted as the deposits of cohesionless sandy debris flows. The abundance of shelf-derived bioclasts within these sediments suggests these flows originated at the shelf break. Some BS-3 deposits are comparable to high-density turbidites as described by Lowe (1979). Deposition of BS-3 sand cored in PC20 from the Bass Canyon is discussed in Section 3.6.

3.4. Intraclastic calcarenite (IQS) and (IMS)

Facies IQS and IMS are massive, poorly-sorted, intraclastic, quartzose calcarenite or calcirudite sediments. They have sharp erosional bases and are associated with V-shaped tributary canyons. Facies IQS is mud-free, often clast-supported and is the predominant cored sediment type found within the steep canyon head of the Anemone Canyon. Facies IMS is mud-rich and matrix-supported and known only from PC19 cored from 3137 m depth near the confluence of

Mudskipper and Moray canyons. (Table 1, Figs. 11C, 12B and 13A,D).

The chaotic and coarse-grained nature of these facies suggests they were deposited rapidly out of high-energy, sediment gravity flows. Facies IQS sediments are interpreted as the deposits of erosive cohesionless sandy debris flows. These deposits entrained well-cemented lithoclasts from the erosion of older strata. Bathymetric data of the seafloor near PC14 and PC15 in Anemone Canyon show that gradients frequently exceed the angle of repose (>35°) making this area susceptible to slides and slumps. Therefore, mass-wasting is a likely cause of flow initiation. Facies IMS sediments are interpreted as the deposits of cohesive debris flows. All intraclasts cored within PC19 are composed of (unconsolidated) muddy calcarenite (Facies MS), which is rare deeper than the middle slope. Thus, it likely that this flow was derived by mass-wasting of weakly lithified sediment on canyon walls above the middle slope. Matrix strength and confinement of the flow within the canyon could have prevented dispersion allowing the flow to remain cohesive until the flow froze (Shanmugam, 1996).

3.5. Additional facies

Present in small volumes is a bryozoan–molluscan muddy calcarenite facies ((BM)MS) cored from upper slope and low-gradient canyon head environments (Table 1, Fig. 12A) and interpreted as deposits of near-situm biogenic production. Additionally, foraminiferal calcilutite (Facies (F)M) was cored on the Bass Canyon floor and lower slope environments (Table 1, Figs. 13B and 14, 15B). This is interpreted as the primary deposition of hemipelagic mud and planktonic foraminifera.

3.6. FR11/98 piston core stratigraphy

Four Middle to Late Pleistocene nannofossil ages (CN14b–CN15) were assigned to samples from the base of four *FR11/98* piston cores (Shafik, 2000). These are; PC06 and PC17, Subzone CN14b (470–268 ka); PC28 Zone CN15 (140–73 ka); and PC20 lower Zone CN15 (268–140 ka). Li (2004) identified a warming event at 1.6 m from top of core in PC26, although the data resolution was considered low. This event is marked by a decline in the cool-water planktonic *Globigerina bulloides* and an increase in the warm-water planktonic *Globigerinoides ruber* and is likely to represent warming from the last glacial maximum at 18 ka. Correlation between the *FR11/98* piston cores is aided by magnetic susceptibility (MagSus) logs. Correlations were particularly good between the slope facies within PC30 and PC28 and the sand unit cored in PC20 from the Bass Canyon (Figs. 2 and 16).

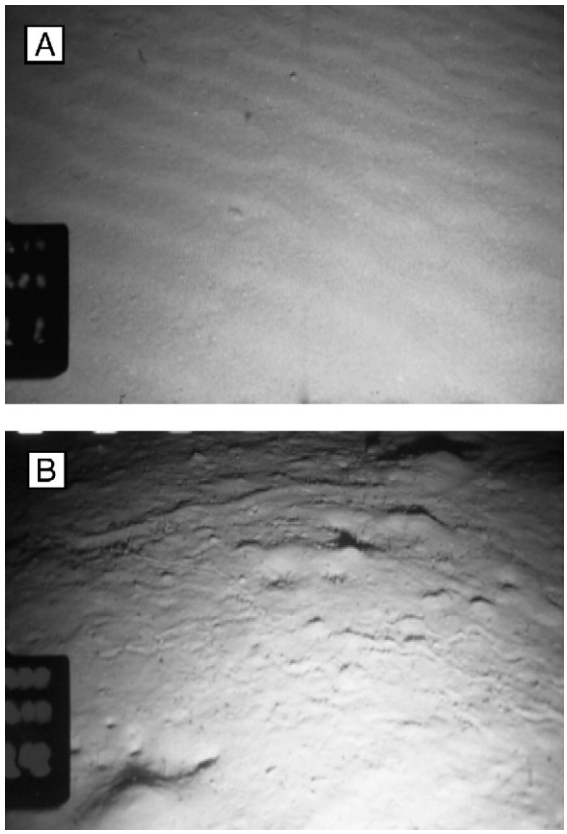

Fig. 15. Seafloor bottom photographs taken during the *FR11/98* cruise. A. Ripples on sandy substrate in the upper reaches of Anemone Canyon head at 250 m depth (BP1 at S38° 44.34, E 148° 21.32). B. Bioturbated mud on the Bass Canyon floor at 3710 m depth (BP5 at S38° 47.58, E149° 29.36).

The MagSus log of PC20 is strongly cyclic, revealing two major saw-toothed cycles (Fig. 17). The preliminary analysis of planktonic foraminifera within high MagSus versus low MagSus regions of these cycles suggest that magnetic variability is related to regional temperature changes. The cool-water planktonic foraminifera *Neogloboquadrina pachyderma* is more abundant within samples from high MagSus zones compared to low MagSus zones (Fig. 17). The nanno-fossil date (CN15, 140–268 ka) obtained by Shafik (2000) from near the base of PC20 suggests these cycles are likely to correspond to the last two Northern Hemisphere glacial eustatic cycles.

A comparison between the mid-latitude stack $\delta^{18}O$ curve of Bassinot et al. (1994) and the MagSus curve of

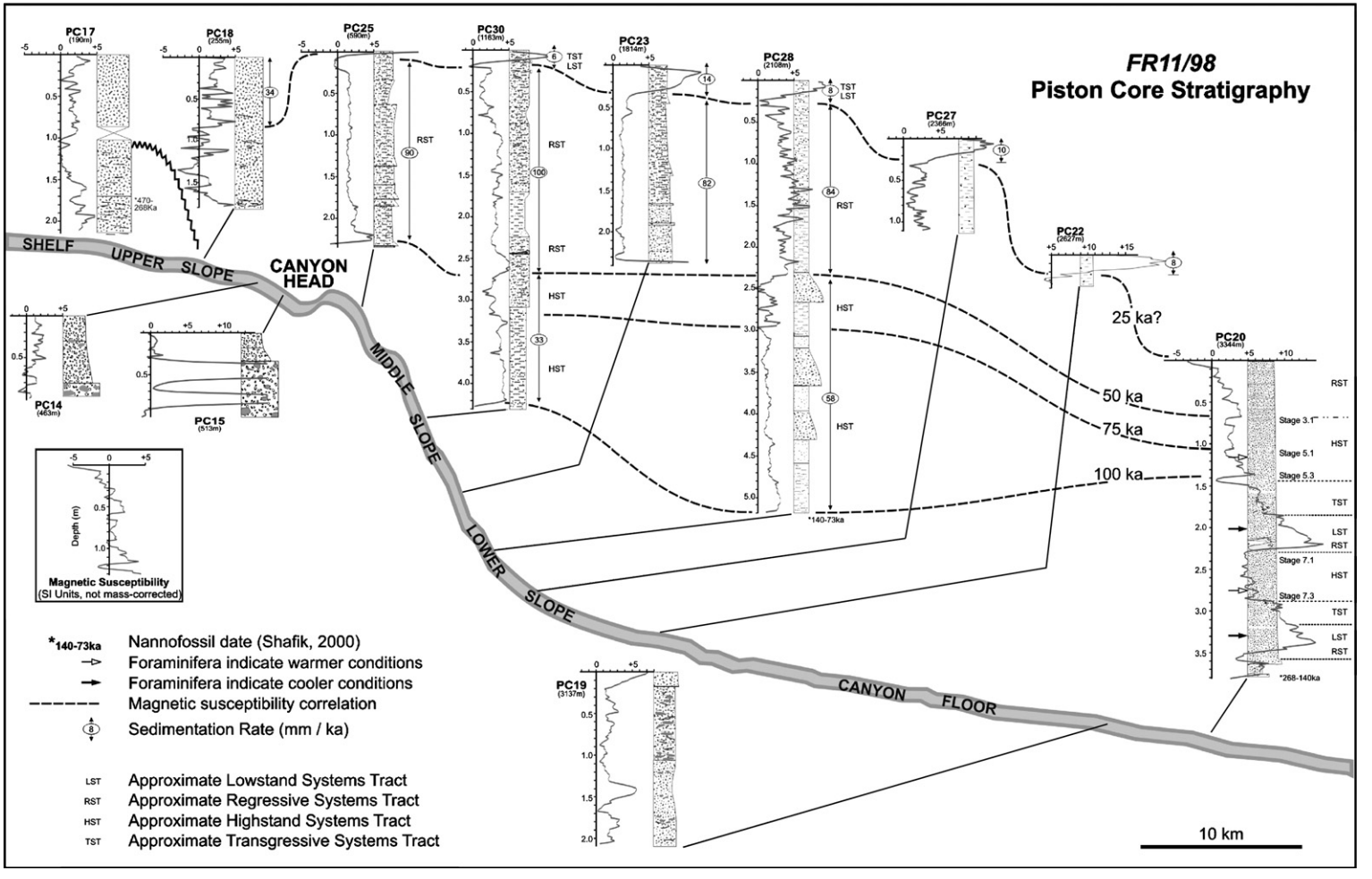

Fig. 16. Correlation diagram for *FR11/98* piston cores, aided by magnetic susceptibility curves. Chronology based nannofossil dates (Shafik, 2000) from base of core samples in PC20, PC28 and PC17, and correlation of magnetic cycles to the low-latitude $\delta^{18}O$ curve (Fig. 17).

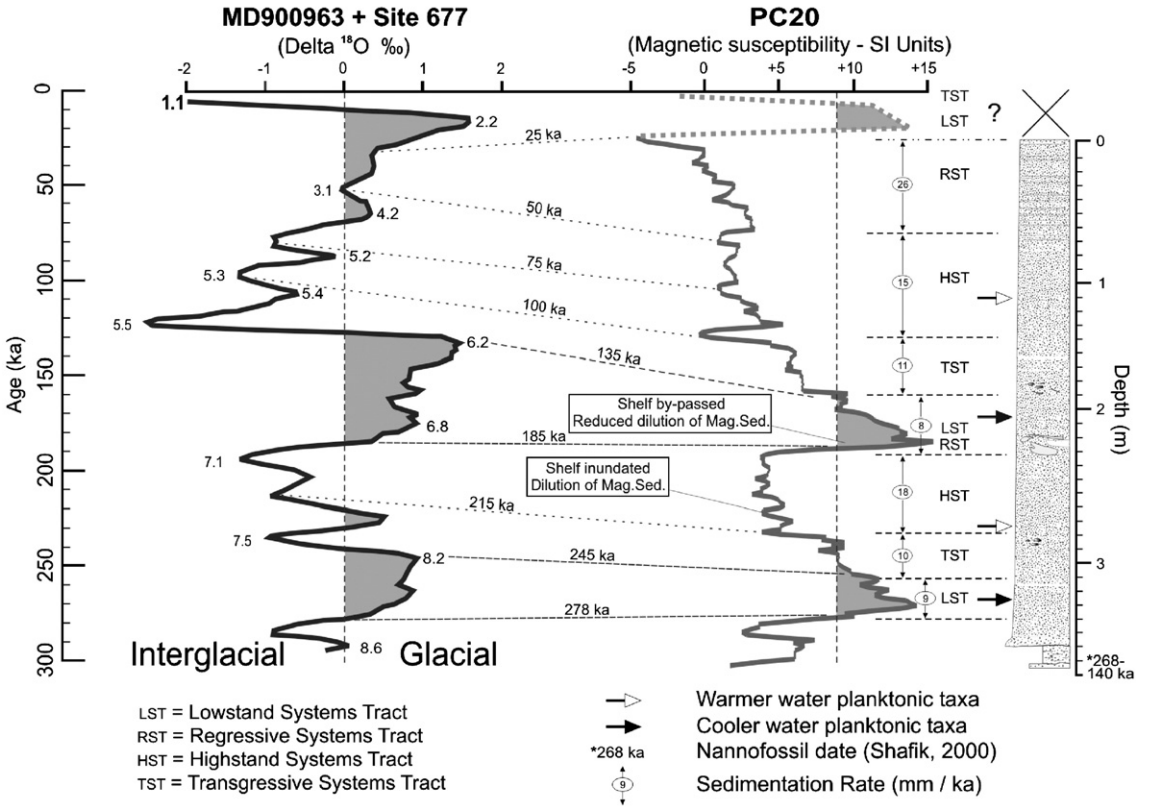

Fig. 17. Correlation of the magnetic susceptibility curve for *FR11/98* piston core PC20 to the stacked low-latitude δ^{18}O curve (MD900963 + ODP site 677). Chronology is that published by the European Project for Ice Coring in Antarctica (EPICA, 2004).

PC20 shows a strong correlation, suggesting that magnetic variability in near-surface sediments of the offshore Gippsland Basin is related to relative sea-level. We tentatively correlate the high MagSus and increase in cool-temperature planktonic taxa at 2.2 m and 3.3 m (from top of core) in PC20 with oxygen isotope stages (OIS) 6.2–6.8 (135–185 ka) and 8.2–8.8.4 (245–278 ka) respectively (Fig. 17). The low MagSus peaks at 1.4 m and 2.7 m are tentatively correlated with OIS 5.3 (98 ka) and 7.1–7.3 (195–215 ka) respectively. The high MagSus peak observed at the top of almost all piston cores has been correlated to the last glacial maximum. This peak is not present in PC20 and is likely to have been eroded or was never deposited. Ages shown in Fig. 17 are from the mid-latitude stack δ^{18}O curve published by the European Project for Ice Coring in Antarctica (EPICA) community (2004) and are used as a guide for calculating sedimentation rates across the basin and to analyses the effects of eustasy on sedimentation, discussed in Section 4.4 below.

The cyclic nature of sand cored in PC20 indicates that deposition was not instantaneous, such as by a turbidite, but was semicontinuous representing slow accumulation over the last ~ 280 ka — probably within a sand stream or channel. The presence of stream-like features coalescing within and travelling down the Bass Canyon from tributary canyons on backscatter data (Fig. 6) supports this idea. The origin of magnetic susceptibility and its cyclic nature is discussed further in Section 4.3.

4. Discussion

The following two sections discuss the evolution of the modern Bass Canyon system from high resolution bathymetry and backscatter data, ground truthed with piston core and surface sediment samples. The variety of canyon forms present within the basin from ‘pre-canyon rills’ (Pratson and Coakley, 1996) to ‘abandoned’ canyons (McGregor et al., 1982) offers a unique opportunity to evaluate canyon evolution. Emphasis is placed on the relationship between canyon head development, canyon profile, and spacing of canyons across the slope. We do not, however, discuss the

formation of the larger and probably much older Bass Canyon, as this is likely to have formed during the early Cenozoic (Hill et al., 1998).

4.1. Canyon initiation and the immature canyon phase

Shepard and Dill (1966) and Shepard (1981) suggested that submarine canyons result from the long-time persistence of multiple processes, which may include a variety of marine processes, tectonics, biological activity, subaerial exposure and fluvial incision. Of these processes, tectonics is unlikely to be of significance for recent canyon development in the Gippsland Basin, due to the relatively stable nature of the continental margin. Biological activity, particularly molluscan and bryozoan productivity, is of major significance to sedimentation rates and thus slope stability. The effects of fluvial processes and relative sea level on canyoning are discussed below.

Many early researchers stressed the importance of rivers and relative sea level fall in the formation of submarine canyons, suggesting that modern canyons relate to modern river systems (Boutakoff, 1963; Hopkins, 1966). This idea became popularised following the advent of the sequence stratigraphic model (Van Wagoner et al., 1988), which reasoned that fluvial incision and canyoning of the shelf and upper slope would be expected during lowstand. However, studies from the North American east coast Atlantic canyons (Twichell and David, 1982) showed that many modern canyons are slope-confined, and have heads that terminate in water depths well below Quaternary lowstand limits. Twichell and David (1982) were the first to propose the fully marine 'headward erosion' model for canyon initiation, which was later developed by Pratson et al. (1994) and Pratson and Coakley (1996).

Many tributary canyons of the modern Bass Canyon system currently breach the shelf, and therefore, potentially are related to modern river systems in the Gippsland Basin. However, evidence from the high carbonate facies, magnetic imagery and shallow seismic surveys of the Gippsland shelf (Holdgate et al., 2003; Mitchell et al., 2007) show that only one of the modern shelf-breaching tributary canyons (Anemone Canyon, Fig. 18) has had Quaternary fluvial connections. All other tributaries have not, and are unlikely to have had at any time in the late Tertiary. Leach and Wallace (2001) noted that modern canyons offshore from the Otway coast (Australia) are evenly spaced where there are no

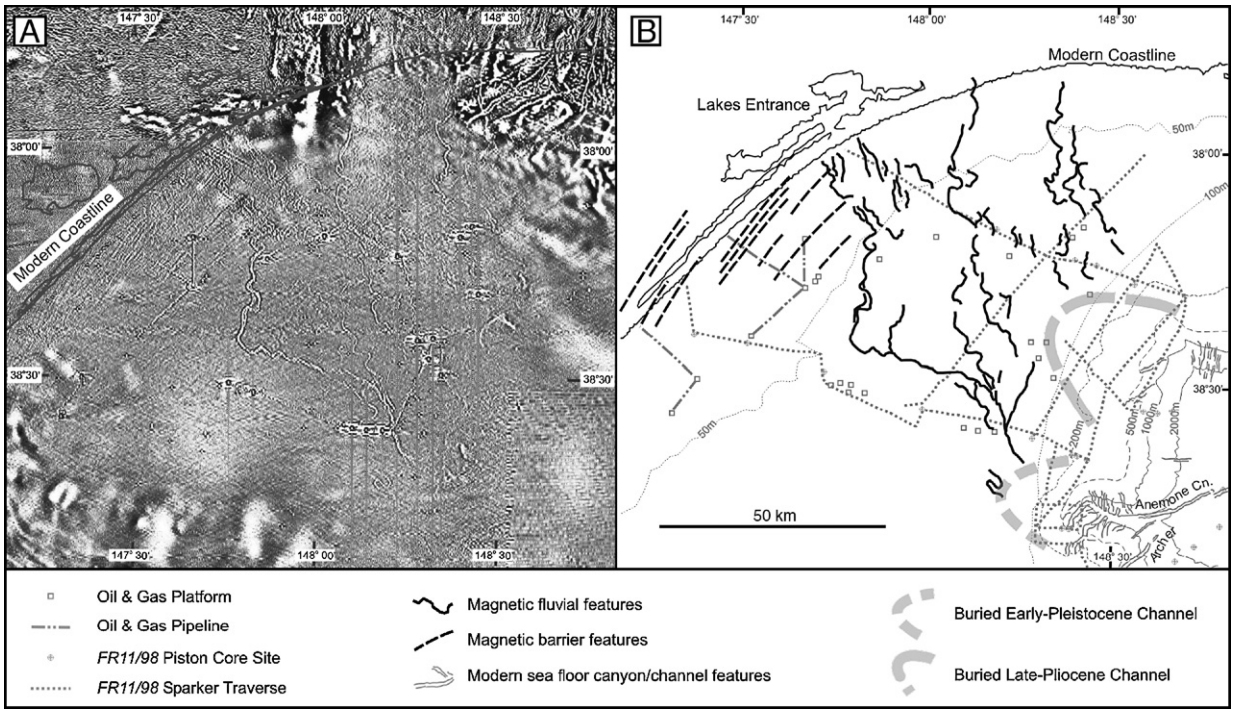

Fig. 18. Simplified interpretation of airborne magnetic imagery of the Gippsland Basin, showing buried magnetic fluvial channels and magnetic barrier features identified by Holdgate et al. (2003), location of buried canyon heads (Mitchell et al., 2007), present-day canyon features, isobaths, and major petroleum platforms and pipelines. Image courtesy of the Geological Society of Victoria. Light pixels equate to high magnetic regions.

onshore river systems, indicating that in a dominantly cool-carbonate setting, canyoning is likely to be a fully marine process. Furthermore, shallow seismic data (Mitchell et al., 2007) identifies that the fluvial connection between the Anemone Canyon and the Mitchell/Thompson river systems post-date the existence of the shelf-breaching Anemone Canyon. The subsequent fluvial connection to the Anemone Canyon was aided by the presence of a shallow seafloor depression overlying buried Pliocene (and older) canyon structures (Figs. 3 and 18), which diverted the lowstand river systems to the canyon head. Thus, all the modern tributary canyons within the Gippsland Basin were probably initiated by marine processes alone.

Piston core and surface sediment data from this study suggest that the main process causing canyon initiation and growth within the Gippsland Basin is downslope-eroding sediment gravity flows, as recognised by Fukushima and Pantin (1985) and Pratson et al. (1994). Such flows are derived from over-steepened shelf break sediments, and are likely to be triggered by high sedimentation rates and the Bass Cascade density current. If mass-wasting processes were a significant part of the canyon initiation process in the Bass Canyon system, we would expect to see widespread depositional evidence for this in piston core and bathymetry data, particularly on and below steep slope regions. This is not the case. In fact, sediments observed from piston core and bathymetry data from across the middle- and lower slope lack cohesive debris flow or slump deposits and slump or scar structures. Instead, sediments cored on the middle slope are comprised of low-energy mud flow deposits (Fig. 11A) indicative of slow creep or low-energy cohesive flows. Evidence for mass-wasting is only present within shelf-breaching tributary canyons that already have very well-developed, deeply incised, dendritic canyon heads (Figs. 2, 8, 11C, 12B), suggesting that mass-wasting becomes important as a canyon matures, but is not initially important.

Although linear ridge and channel structures or 'pre-canyon rills' ((Figs. 2, 3 and 5)D) are well-developed on much of the middle slope — many with dimensions comparable to small canyons — it is doubtful that they develop into canyons. Unfortunately, we cannot confirm the existence of immature canyons transitional from 'pre-canyon rills' on the upper slope, as the upper limit of the swath-mapped data is 400–500 m depth. This said, headward erosion cannot be ruled out, as sediments cored on the lower slope below well-developed middle slope channels include cohesionless sandy debris flows (or turbidites) (Fig. 11B), which are comprised largely of shelf-derived bioclasts. This indicates that sediment does bypass the middle slope, probably travelling through the middle slope channels, and could induce headward erosion (as modelled by Pratson and Coakley, 1996).

Seismic evidence from Mitchell et al. (2007) suggests that the deeply-incised canyon head morphology of the modern shelf break was caused by a tripling in shelf (carbonate) sedimentation rates, under highstand conditions in the Late Pliocene, together with a gradual steepening of pre-existing channel walls, which began in the middle Pliocene. The increased sedimentation rates and steepening of channel walls are attributed to strengthening of a shelf-derived (highstand) seasonal density current known as the Bass Cascade (Godfrey et al., 1980), which probably intensified as the Bass Strait shallowed towards the end of the Pliocene (Mitchell et al., 2007). Ripple marks on sandy substrate observed in bottom photographs at depths of 250 m in the upper head of Anemone Canyon support the presence of significant traction currents today (Fig. 15A). Therefore, it is likely that Quaternary canyoning within the Gippsland Basin initiated from downslope-eroding sediment gravity flows triggered at the shelf break on over-steepened sediments by littoral currents and or the Bass Cascade. Sediment flows from multiple tributary canyons (and unconfined slope turbidites) coalesce and flow down the deepwater Bass Canyon (Fig. 6) depositing well-sorted sand (Fig. 14).

Intensification of the northeast flowing Bass Cascade may also explain why the modern Bass Canyon system is so strongly asymmetrical, with all V-shaped canyons occupying only southern slopes, and why only the southern wall of the Anemone Canyon head is deeply incised. Additionally, the Bass Cascade may also explain the northeast orientation of shallow U-shaped channels present on the outer-shelf and upper slope of the central platform (Fig. 2).

4.2. Development of the mature canyon phase and canyon burial

As an immature canyon or channel incises into the shelf break, slope failure within the channel becomes more likely. Sediments of the shelf carbonate factory, which are composed of molluscan and bryozoan sand and gravel, may be transported to the shelf edge by littoral or storm induced currents, or by the Bass Cascade. These sediments are cohesionless, readily mobilised and provide the 'fuel' for self-sustaining and erosive sediment gravity flows (Fukushima and Pantin, 1985). Such flows scour channel floors and steepen walls.

On the steeper middle slope, a slope-confined canyon is most likely to fail at its head, as the gradient of the head wall is more likely to exceed the maximum threshold of failure than the walls. However, on low slope gradients, such as the outer-shelf and upper slope, canyon walls are just as likely to reach the maximum slope threshold as the head, allowing a dendritic canyon head morphology to develop (Fig. 3B). Once a dendritic structure is established, the canyon head captures and funnels larger volumes of shelf sediment into the canyon, and the process becomes self propagating. Widening of the canyon head and entrapment of coarse-grained abrasive sediment leads to an influx of erosional sediment gravity flows, cutting steep-sided V-shaped incisions (Fig. 7B). Large erosive flows propagate canyon growth in the downslope direction over the lower slope, while the development of steep canyon walls promotes mass-failure (evident in piston cores Figs. 11C, 12B and bathymetry data Fig. 8).

The widening of canyon heads across the shelf has further effects on slope processes beyond the canyons. Sediments captured by canyon heads bypass the slope, preventing adjacent middle slope channels (pre-canyon rills) from developing further. This explains the absence of middle slope channels adjacent to canyons with well-developed canyon heads. Additionally, the lateral spacing of canyons across the slope (11 km±3 km, Fig. 2) is related to the width of canyon heads across the shelf. The broader canyon heads are, the greater the lateral distance between canyons. A mature stage canyon will continue broadening at the canyon head until a stable gradient is achieved between the adjacent shelf (or slope) and floor of the canyon. Piston core sediments suggest mass-wasting is still a major sedimentary process within the Anemone Canyon head (the largest canyon head), implying that it has not yet stabilized (Fig. 12B). Once the mature canyon has reached a state of equilibrium with the adjacent shelf or slope, there will be a significant reduction in shelf-derived mass-wasting events and associated large erosional sediment gravity flows. In the absence of such flows, background pelagic sedimentation and the continued prograding of sediments into the canyon trough from adjacent slopes (Wallace et al., 2002) aid in promoting the development of a smoothed U-shaped canyon profile. Continued minor sediment gravity flows may maintain an open canyon system indefinitely and might cause canyon sinuosity (McGregor et al., 1982), as observed in the Everard Canyon (Figs. 2 and 3). Prevailing currents may lead to lateral migration of canyons, found in Miocene to recent canyons from the adjacent Otway Basin (Leach and Wallace, 2001) and Pliocene canyons in the Gippsland Basin (Mitchell et al., 2007).

The abandonment of canyons is likely to follow a major change in the sediment supply regime, such as a shift of depo-centre away from the canyon head (Pratson et al., 1994). Such a shift may result from a rapid (glacially forced) eustatic fluctuation, a reversal in longshore or deepwater currents, or a structural event that diverts sediment elsewhere. The most likely scenario in the Gippsland Basin would be a shift or decline in productivity of the major carbonate factories, probably caused by less favourable oceanic conditions or by lowstand exposure of the shelf, which would reduce the optimal molluscan and bryozoan habitats. Sedimentation at the canyon heads, in all canyons not capturing a lowstand river, would then be limited to hemipelagic settling, allowing an in-filled low-relief broad canyon head morphology to develop. Seafloor morphology observations suggest that the Everard Canyon is in this stage. However, at present, shelf sediments appear to be advancing towards the head of the Everard Canyon (Figs. 2–4), possibly transported by a strengthening (longshore) East Australian Current, which may reactivate the Everard Canyon.

Stabilisation of the canyon heads allows subsequent (slow) progradation to in-fill canyons progressively in the downslope direction, resulting in slope-confined U-shaped remnant canyons, such as, the lower slope confined canyons on the northern slopes (Whaleshark, Sole and Shark, Fig. 2).

4.3. Eustasy and the origin of high magnetic susceptibility sediments

Magnetic imagery of the Gippsland shelf (Fig. 18) reveals a complex system of high-magnetic meandering channels beneath shallow subsurface sediments, not expressed on the modern seafloor. Holdgate et al. (2003, P. 415, Fig. 12) showed that the origins of these channels are the modern Tambo and Nicholson rivers, Ironstone Creek, and Snowy River systems, and interpret them as Pleistocene lowstand fluvial features. Their strong magnetic signature was suggested to be caused by ferruginous cementation. Fluvial channels drained towards the south-southeast, initially following the approximate axis of the basin, but were then directed down shallow seafloor depressions overlying much older buried Pliocene canyons and towards the modern Anemone Canyon. This indicates that there was at least one direct fluvial-canyon connection during the more extreme Pleistocene lowstands, which has significant implications

for shelf/slope bypassing and sediment supply to the deep-water environment.

High MagSus variability recorded within slope and canyon piston cores, is likely to be caused by an influx of fluvial (or aeolian) ferruginous particles. Intensification of northern hemisphere glaciations during the Late Pliocene and Pleistocene led to the development of vast tracts of mobile dune-fields, sand-plains, and the displacement of warm-wet forests with cool-dry open vegetation over much of the interior of Australia (Wasson, 1984; Gallagher et al., 2003; Cupper, 2005). Dry (glacial/lowstand) climates and predominantly open vegetation environments are likely to support an increase in terrigenous (more ferruginous) particles to the deepwater sedimentary environment by increasing total input volumes of aeolian-derived particles, and by allowing fluvial sediments to bypass the shelf at extreme lowstand to enter canyon heads directly.

The dramatic shift from low to high MagSus measured at 2.3 and 3.4 m in piston core PC20 is likely to represent extreme lowstand eustatic conditions where direct fluvial — canyon connection or complete shelf-bypassing (Fig. 17) occurred, allowing siliciclastic ferruginous particles to enter the canyon system and slope without dilution from shelf carbonates. Remnant lowstand shelf accumulations of aeolian or fluvial ferruginous particles would be gradually diluted as carbonate production increased under highstand conditions, resulting in a gradual up-core decrease in MagSus, as is observed in PC20 following each MagSus high.

4.4. Sedimentation rates and the effects of Pleistocene eustasy

A sequence stratigraphic framework has been developed based on the correlation between MagSus variation in piston cores and the MD900963+ODP677 δ^{18}O stack (Section 3.6, Fig. 17) allowing sedimentation rates and depositional processes to be tentatively analysed during various systems tracts. Sedimentation across much of the shelf during the Pleistocene was episodic as large eustatic fluctuations frequently exposed the shelf during the onset of Northern Hemisphere glaciations (Holdgate et al., 2003). Deposition in canyon heads was extremely localised with many regions undergoing net erosion (Mitchell et al., 2007). With the exception of the last glacial lowstand and subsequent transgression (last 25 ka), mixed muddy calcarenite, sandy calcilutite and calcarenite accumulated on the upper and middle slope at rates of 33–100 mm/ka, and on the lower slope at rates of 58–84 mm/ka, while calcarenite accumulated in sand channels on the floor of the Bass Canyon under semicontinuous deposition at 8–26 mm/ka.

The highest sedimentation rates are recorded in sections of core where upwardly decreasing MagSus is correlated to gradually decreasing values in δ^{18}O (OIS 3.1–2.2). These sediments are inferred to have been deposited in the regressive systems tracts (RST). Upper to lower slope RST sedimentation rates range from 82–100 mm/ka, while on the Bass Canyon floor, sedimentation rates for PC20 reached their maximum at 26 mm/ka. Conversely, the lowest sedimentation rates are recorded in core associated with the highest MagSus measurements, correlated to high δ^{18}O values (OIS 2.2, 6.2–6.8 and 8.2–8.4) and in core with rapidly decreasing MagSus, correlated with rapid decreases in δ^{18}O values (OIS 2.2–1.1, 6.2–5.5, 8.2–7.5). These sediments are inferred to have been deposited during the lowstand systems tracts (LST) and transgressive systems tracts (TST) respectively. During the LST and TST, slope sediments accumulated at 6–14 mm/ka, while sand in Bass Canyon (PC20) accumulated at 8–10 mm/ka. Moderate to high sedimentation rates are recorded for core associated with low MagSus measurements, which are correlated to low δ^{18}O values (OIS 3.1–5.3 and 7.1–7.5) and are inferred to have been deposited during highstand systems tracts (HST). During the HST, slope sediments accumulated at 33–58 mm/ka, while Bass Canyon sands accumulated at 15–18 mm/ka.

4.5. Cool-water carbonate-dominant vs siliciclastic-dominant canyon systems

Sediments of the Gippsland Basin are derived largely from the mechanical and biological breakdown of molluscs and bryozoans on the shelf, and as such, they can be treated similar to sediments in siliciclastic environments. However, two important differences should be accounted for between terrigenous- and carbonate-dominant sediments. Firstly, carbonate grains are generally more porous and irregularly shaped than quartz, feldspathic or other lithic grains. As such, carbonate grains are more readily mobilised and transported, suggesting that cool-water carbonate systems are more sensitive to, and should respond faster to, changing oceanographic conditions than siliciclastic systems. Secondly, carbonate sediments are prone to early diagenetic processes that may lithify sediments, thus increasing the slope failure threshold, allowing steeper morphologies to be obtained. However, there is little evidence for early diagenetic lithification within

the *FR11/98* piston cores, suggesting that over steepening, promoted by early diagenesis, is not a significant factor here.

4.6. Low backscatter acoustic properties within canyons

Canyons are generally associated with higher than average return-strength signals, believed to be produced by hard, rough and scoured surfaces, boulder and pebble trails, and coarse-grained sediments (Kenyon et al., 2002; Hill et al., 2005). However, many canyons within the Gippsland Basin have subtly lower return-strength acoustics than surrounding slopes. Such areas include much of the floor of the Bass Canyon, the lower slope regions of Mudskipper and Anemone Canyons, the upper- and middle slope regions of Pisces Canyon, and most of Moray and Archer canyons. The cause of this is unknown. Kenyon et al. (2002) reported similar unexplained acoustic responses from sand lobes at the mouths of canyons off Corsica and Sardinia, attributing thin mud-drapes as the cause of low backscatter. Similar thin mud-veneers may drape such canyon regions in the Gippsland Basin. This, however, would indicate recent inactivity in canyons.

The numerous stream-like low backscatter features identified on the Bass Canyon floor and its tributaries (Fig. 6) suggests that the canyons are active. Alternatively, we suggest that low backscatter sediments might be produced by particularly smooth seafloor surfaces on fine sand- and silt-dominated substrates, which might be formed by regular low-energy sediment gravity flows or currents and a lack of surface irregularities caused by bioturbation or marine life.

5. Conclusions

- High resolution bathymetry of the Bass Canyon system reveals five major shelf-breaching tributary canyons and three slope-confined canyons, which coalesce at the head of the Bass Canyon at 3000 m depth; one shelf-breaching canyon that terminates at the middle/lower slope boundary and many (predominantly) middle slope channels present in regions distal to shelf-breaching tributary canyons. This study recognises that the diversity in canyons and channels present in the Quaternary Gippsland Basin represent stages in canyon development and evolution. Five significant stages are recognised:
  1. *V-shaped linear channels* that develop on the middle slope. These may evolve into canyons through headward erosion.
  2. Shelf-breaching *immature tributary canyons* that have not yet developed dendritic canyon heads.
  3. Shelf-breaching *V-shaped mature tributary canyons* that have deeply incised unstable dendritic canyon heads.
  4. Shelf-breaching *U-shaped mature tributary canyons* that have stable, low-relief dendritic canyon heads.
  5. Slope-confined *abandoned tributary canyons* that have broad U-shaped profiles and non-dendritic canyon heads.
- The predominant shelf sediment is quartzose, bioclastic calcarenite and molluscan shell gravel deposited under the influence of wave base. Slope sediment is predominantly muddy calcarenite and sandy calcilutite deposited by mud flows, sandy debris flows, and from hemipelagic settling. The predominant canyon sediment consists of well-sorted calcarenite and intraclastic-calcarenite deposited by cohesionless sediment gravity flows. Rare intraclastic sandy calcilutite is present, deposited by cohesive debris flows.
- Highest sedimentation rates occurred across slope (82–100 mm/ka) and canyon environments (26 mm/ka) during the RST, while moderate rates occurred during the HST at 33–58 mm/ka on slopes and 15–18 mm/ka within the Bass Canyon. The lowest sedimentation rates occurred during the LST and TST with slope sediments accumulating at 6–14 mm/ka and Bass Canyon sands accumulating at 8–10 mm/ka.
- The Bass Cascade density current is of regional importance in the development of canyons and is likely to be responsible for triggering sediment gravity flows at the shelf break and producing the strong asymmetry observed in the Quaternary Bass Canyon system.

Acknowledgements

The authors wish to thank Geoscience Australia for providing bathymetry data for the Gippsland Basin. The Department of Industry, Technology and Environment (Geological Society of Victoria) for permission to use the airborne magnetic image of the Gippsland Basin. Thanks to Jock Keene and Dave Mitchell of The University of Sydney, Ocean Drilling Program for safely storing the *FR11/98* piston cores. Thanks to Warren Dickinson (Victoria University of Wellington), Mark Lloyd Davies (Universiteit van Amsterdam) and particularly Gordon Holm (The University of Melbourne) for the advice and services with regards to soft-

sediment impregnation and thin-section preparation. Thanks to Peter Hill for the valuable conversations regarding backscatter acoustics, and reviewer/editor David Piper for helpful comments and suggestions. The *RV Franklin* cruise was partially funded by the ARC Research Grant No. A39803024.

References

Bacelle, L., Bosellini, A., 1965. Diagrammi per la stima visiva della composizione percentuale nelle rocce sedimentarie. Sci. Geol. Paleont. 1 (3), 59–62.

Bassinot, F.C., Labeyrie, L.D., Vincent, E., Quidelleur, X., Shackleton, N.J., Lancelot, Y., 1994. The astronomical theory of climate and the age of the Brunhes–Matuyama magnetic reversal. Earth Planet. Sci. Lett. 126, 91–108.

Bernecker, T., Partridge, A.D., Webb, J.A., 1997. Mid-late Tertiary deep-water temperate carbonate deposition, offshore Gippsland Basin, southeastern Australia. In: James, N.P.C., Jonathan A.D. (Eds.), Cool-water carbonates, vol. 56. Geelong, Victoria, Australia, SEPM (Society for Sedimentary Geology), Tulsa, OK, United States (USA), p. 221–236.

Bertoni, C., Cartwright, J., 2005. 3D seismic analysis of slope-confined canyons from the Plio-Pleistocene of the Ebro Continental Margin (Western Mediterranean). Basin Res 17, 43–62.

Boutakoff, N., 1963. The geology and geomorphology of the Portland area. Mem. Geol. Surv. Victoria 22.

Colwell, J.B., Coffin, M., et al., 1987. RigSeismic research cruise 13: northeast Gippsland Basin and southern New South Wales margin — initial report: Canberra, Bureau of Mineral Resources. Geol. Geophys. Rep. 283.

Conolly, R., 1968. Submarine canyons of the continental margin, East Bass Strait (Australia). Mar. Geol. 6, 449–461.

Cupper, M.L., 2005. Last glacial to Holocene evolution of semi-arid rangelands in southeastern Australia. Holocene 14, 541–553.

Davies, P.J., 1979. Marine geology of the continental shelf off southeast Australia Bureau of Mineral Resources, Geology and Geophysics Bureau of Mineral Resources. Geol. Geophys. BMR Bull. 195.

Davies, P.J., Marshall, J.F., 1973. BMR marine geology cruise in Bass Strait and Tasmanian waters, vol. 1973/134. Bureau of Mineral Resources, Geology and Geophysics Record.

EPICA, 2004. Eight glacial cycles from an Antarctic ice core. Nature 429, 623–628.

Exon, N.F., Hill, P.J., Keene, J.B., Smith, S.M., 1999. The "SOJOURN 7" Swath-Mapping Cruise of R.V. Melville off eastern Tasmania and in the Gippsland Basin. AGSO Record 1999/7 Record 1999/7, pp. 1–50.

Exon, N.F., Hill, P.J., Patridge, A., Chaproniere, G.C., Keene, J.B., 2002. Cretaceous Volcanogenic and Miocene Calcareous Strata Dredged From the Deepwater Gippsland Basin on R/V Franklin Research Cruise FR11/98: Canberra, Geoscience Australia— Petroleum and Marine Division Record 2002/07, p. 56.

Farre, J.A., McGregor, B.A., Ryan, W.B.F., Robb, J.M., 1983. Breaching the shelfbreak: passage from youthful to mature phase in submarine canyon evolution. In: Stanley, D.J., Moore, G.T. (Eds.), The Society of Economic Paleontologists and Mineralogists. The Shelfbreak: Critical Interface on Continental Margins, vol. 33, pp. 25–39.

Feary, D.A., Loutit, T.S., 1998. Cool-water carbonate facies patterns and diagenesis — the key to the Gippsland Basin 'velocity problem'. AAPEA J. 38, 137–145.

Fukushima, Y.P.G., Pantin, H.M., 1985. Prediction of ignitive turbidity currents in Scripps submarine canyon. Mar. Geol. 67, 55–81.

Gallagher, S.J., Greenwood, D.R., Taylor, D., Smith, A.J., Wallace, M.W., Holdgate, G.R., 2003. The Pliocene climatic and environmental evolution of southeastern Australia: evidence from the marine and terrestrial realm. Palaeogeogr. Palaeoclimatol. Palaeoecol. (PALAEO) 193, 349–382.

Godfrey, J.S., Jones, I.S.F., Maxwell, J.G.H, Scott, B.D., 1980. On the Winter Cascade from Bass Strait into the Tasman Sea Australian. J. Mar. Freshw. Res. 31, 275–286.

Harris, P., Radke, B., Smith, A., Glen, K., Rollet, N., Exon, N., Passlow, V., 2000. Marine Geological Data Collected During Southern Surveyor Voyage 001/00: Eastern Bass Strait and Great Australian Bight, (AGSO Research Cruise No. 224) AGSO Record 2000/43.

Henry, W.C., Hyden, A.M., Williams, S.L., 2000. Innovations in subsea development and operation. APPEA J. 40, 439–449.

Hill, P.J., Exon, N.F., Keene, J.B., Smith, S.M., 1998. The continental margin off East Tasmania and Gippsland; structure and development using multibeam sonar data. In: Rajagopalan, S., Pettifer, G. (Eds.), ASEG 13th international Geophysical Conference and Exhibition; Conference Papers, vol. 29. Melbourne, Exploration Geophysics, pp. 410–419.

Hill, P.J., De Deckker, P., Exon, N.F., 2005. Geomorphology and evolution of the gigantic Murray canyons on the Australian southern margin. Aust. J. Earth Sci. 52, 117–136.

Holdgate, G.R., Wallace, M.W., Daniels, J., Gallagher, S.J., Keene, J.B., Smith, A.J., 2000. Controls on Seaspray Group sonic velocities in the Gippsland Basin — a multi-disciplinary approach to the canyon seismic velocity problem. APPEA J. 40, 295–313.

Holdgate, G.R., Wallace, M.W., Gallagher, S.J., Smith, A.J., Keene, J.B., Moore, D., Shafik, S., 2003. Plio-Pleistocene tectonics and eustasy in the Gippsland Basin, southeast Australia: evidence from magnetic imagery and marine geological data. Aust. J. Earth Sci. 50, 403–426.

Hopkins, B.M., 1966. Submarine canyons, The B.H.P. Technical Bulletin 26 v. 10, 39–43.

James, N.P., Collins, L.B., Bone, Y., Hallock, P., 1999. Subtropical carbonates in a temperate realm. Modern sediments on the southwest Australian Shelf. J. Sediment. Res. 69, 1297–1321.

Jones, H.A., Davies, P.J., 1983. Superficial sediments of the Tasmanian Continental shelf and part of Bass Strait: Canberra, Bureau of Mineral Resources. Geology and Geophysics. BMR Bulletin, vol. 218.

Keene, J.B., 1998. Cruise summary R/V Franklin FR11/98 CSIRO Marine Research. Hobart.

Kenyon, N.H., Klaucke, I., Millington, J., Ivanov, M.K., 2002. Sandy submarine canyon-mouth lobes on the western margin of Corsica and Sardinia, Mediterranean Sea. Mar. Geol. 184, 69–84.

Leach, A.S., Wallace, M.W., 2001. Cenozoic submarine canyon systems in cool water carbonates from the Otway Basin, Victoria, Australia. In: Hill, K.C., Bernecker, T. (Eds.), PESA — Eastern Australasian Basins Symposium. PESA, Melbourne, Victoria.

Levitas, S., 1982. Climatological atlas of the world oceans National Oceanic and Atmospheric Administration. Prof. Pap. 13.

Li, C., 2004. Palaeoceanography of the Australian region during the Last Glacial Maximum: A planktonic foraminiferal view [Honours thesis]: Melbourne, University of Melbourne.

Li, F., Dyt, C., Griffiths, C.M., Jenkins, C., Rutherford, M., Chittleborough, J., 2005. Seabed sediment transport and offshore pipeline risk in the Australian southeast. AAPEA J. 45, 523–534.

Lowe, D.R., 1979. Sediment gravity flows: their classification and some problems of application to natural flows and deposits. In: Doyle, L.J., Pilkey Jr., O.H. (Eds.), Geology of Continental Slopes. Special Publication, vol. 27. SEPM, Tulsa, Oklahoma.

Mays, C., 2001. The Pliocene to Recent Palaeoenvironmental Evolution of the Gippsland Basin [Honours thesis]: Melbourne, University of Melbourne.

Marshall, N.G., 1988. A Santonian dinoflagellate assemblage from the Gippsland Basin, Southeastern Australia, Association of Australasian Palaeontologists. Memoir 5, 195–215.

Martinez, J.I., 1994. Late Pleistocene palaeoceanography of the Tasman Sea. Implications for the dynamics of the warm pool in the western Pacific. Palaeogeogr. Palaeoclimatol. Palaeoecol. 112, 19–62.

McGregor, B.A., Stubblefield, W.L., Ryan, W.B.F., Twichell, D.C., 1982. Wilmington Submarine Canyon: a marine fluvial-like system. Geology 10, 27–30.

McMinn, A., 1992. Pliocene through Holocene dinoflagellate cyst biostratigraphy of the Gippsland Basin, Australia. In: Head, M.J.W., John, H. (Eds.), American Association of Stratigraphic Palynologists Foundation. Publishers Press, Salt Lake City, pp. 147–161.

Mitchell, J.K., Holdgate, G.R., Wallace, M.W., Gallagher, S.J., 2007. The Pliocene–Pleistocene history of the Gippsland Basin outer shelf and canyon heads, Southeast Australia. Aust. J. Earth Sci. 54 (1).

Moore, D.H.W.D., 2002. Eastern and Central Gippsland Basin, Southeast Australia; basement interpretation and basin links. Victorian initiative for minerals and petroleum. Department of Natural Resources and Environment Victorian Initiative for Minerals and Petroleum. Report, vol. 69, p. 52.

Passlow, V., 1997. Slope sedimentation and shelf to basin transfer: a cool-water carbonate example from the Otway Margin, Southeast Australia. In: James, N.P.C., Jonathan, A.D. (Eds.), SEPM, vol. 56. SEPM, pp. 107–125.

Pratson, L.F., Coakley, B.J., 1996. A model for the headward erosion of submarine canyons induced by downslope-eroding sediment flows. GSA Bull. 108, 225–234.

Pratson, L.F., Ryan, W.B.F., Mountain, G.S., Twichell, D.C., 1994. Submarine canyon initiation by downslope-eroding sediment flows; evidence in late Cenozoic strata on the New Jersey continental slope. Geol. Soc. Amer. Bull. 106, 395–412.

Rahmanian, V.D., Moore, P.S., Mudge, W.J., Spring, D.E., 1990. Sequence stratigraphy and the habitat of hydrocarbons, Gippsland Basin, Australia. In: Brooks, J. (Ed.), Classic Petroleum Provinces, vol. 51. Geological Society of London Special Publication, London, pp. 525–541.

Schneider, P.M., 1985. Report on SP4 maps on the sediments, morphology, and acoustic properties of the southwest Pacific seafloor: Sydney, Ocean Sciences Institution of Sydney University Report 15.

Shafik, S., 2000. Calcareous Nannofossil Biostratigraphic Assessment of Subsurface Samples from offshore Gippsland Basin, SE Australia, StratSolutions Pty Ltd Vic2000/02.

Shanmugam, G., 1996. High density turbidity currents: are they sandy debris flows? J. Sediment. Res. 66, 2–10.

Shepard, F.P., Dill, R.F., 1966. Submarine canyons and other sea valleys, Rand McNally & Company.

Smith, G.C., 1982. A review of the Tertiary–Cretaceous tectonic history of the Gippsland Basin and its controls on coal measure sedimentation. Aust. Coal Geol. 4, 1–38.

Smith, A.J., Gallagher, S.J., 2003. The Recent foraminifera and facies of the Bass Canyon: a temperate submarine canyon in Gippsland, Australia. J. Micropalaeontol. 22, 63–83.

Smith, A., Gallagher, S.J., Wallace, M.W., Holdgate, G.R., Daniels, J., Keene, J., 2001. The recent temperate foraminiferal biofacies of the Gippsland Shelf: an analogue for Neogene environmental analysis in southeastern Australia. J. Micropalaeontol. 20, 127–142.

Twichell, D.C., David, G. Roberts, 1982. Morphology, distribution, and development of submarine canyons on the United States Atlantic continental slope between Hudson and Baltimore Canyons. Geology 10, 408–412.

Van Wagoner, J.C., Posamentier, H.W., Mitchum, R.M., Vail, P.R., Sarg, J., Loutit, F., Hardenbol, J., 1988. An overview of the fundamentals of sequence stratigraphy and key definitions. The Society of Economic Paleontologists and Mineralogists. Special Publication, vol. 42.

Veevers, J.J., 1986. Breakup of Australia and Antarctica estimated as mid-Cretaceous (95 Ma). Earth Planet. Sci. Lett. 77, 91–99.

Veevers, J.J., Powell, C., Roots, S.R., 1991. Review of seafloor spreading around Australia. I. Synthesis of the patterns of spreading. Aust. J. Earth Sci. 38, 373–389.

Wallace, M.W., Holdgate, G.R., Daniels, J., Gallagher, S.J., Smith, A., 2002. Sonic velocity, submarine canyons, and burial diagenesis in Oligocene–Holocene cool-water carbonates, Gippsland Basin, southeast Australia. AAPG Bull. 86, 1593–1607.

Wasson, R.J., 1984. Late Quaternary palaeoenvironments in the desert dunefields of Australia. In: Vogel, J. (Ed.), Late Cenozoic Palaeoclimates of Inland Australia. Balkema, Rotterdam, pp. 419–432.

Willcox, J.B., Colwell, J.B., Constantine, A.E., 1992. New ideas on Gippsland Basin regional tectonics. In: Barton, C.M.H.K., Able, C., Foster, J., Kempton, N. (Eds.), Energy, Economics and Environment Gippsland Basin Symposium. AustIMM & PESA, Melbourne, pp. 93–110.